Available online at www.sciencedirect.com
SCIENCE DIRECT®
Journal of Sound and Vibration 267 (2003) 301–334
JOURNAL OF SOUND AND VIBRATION
www.elsevier.com/locate/jsvi

A general linear mathematical model of power flow analysis and control for integrated structure–control systems

Y.P. Xiong[a,b,*], J.T. Xing[b], W.G. Price[b]

[a] *Institute of Engineering Mechanics, Shandong University, Jinan 250061, People's Republic of China*
[b] *School of Engineering Sciences, Ship Science, University of Southampton, Highfield, Southampton, SO17 1BJ, UK*

Received 15 May 2001; accepted 22 October 2002

Abstract

Generalized integrated structure–control dynamical systems consisting of any number of active/passive controllers and three-dimensional rigid/flexible substructures are investigated. The developed mathematical model assessing the behaviour of these complex systems includes description of general boundary conditions, the interaction mechanisms between structures, power flows and control characteristics. Three active control strategies are examined. That is, multiple channel absolute/relative velocity feedback controllers, their hybrid combination and an existing passive control system to which the former control systems are attached in order to improve overall control efficiency. From the viewpoint of continuum mechanics, an analytical solution of this generalized structure–control system has been developed allowing predictions of the dynamic responses at any point on or in substructures of the coupled system. Absolute or relative dynamic response or receptance, transmissibility, mobility, transfer functions have been derived to evaluate complex dynamic interaction mechanisms through various transmission paths. The instantaneous and time-averaged power flow of energy input, transmission and dissipation or absorption within and between the source substructure, control subsystems and controlled substructure are presented. The general theory developed provides an integrated framework to solve various vibration isolation and control problems and provides a basis to develop a general algorithm that may allow the user to build arbitrarily complex linear control models using simple commands and inputs. The proposed approach is applied to a practical example to illustrate and validate the mathematical model as well as to assess control effectiveness and to provide important guidelines to assist vibration control designers.

*Corresponding author: Tel.: +44-23-8059-6549; fax: +44-23-8059-3299.
E-mail addresses: y.p.xiong@ship.soton.ac.uk, xiongyp@sdu.edu.cn (Y.P. Xiong), j.t.xing@ship.soton.ac.uk (J.T. Xing), w.g.price@ship.soton.ac.uk (W.G. Price).

0022-460X/03/$ - see front matter
doi:10.1016/S0022-460X(03)00194-9

1. Introduction

Vibration control problems have received much attention over past decades [1–3]. The control of structural vibrations produced by earthquake, wind, sea waves, explosion, impacts and other vibration sources enhances safety of operation of the overall dynamical system under examination and successful applications of control strategies are found in many branches of engineering, i.e., civil, aerospace, marine, mechatronics [1–3]. In the past, vibration control systems were primarily studied adopting passive control methods such as flexible mounts, elastomeric bearing systems, damping or absorbing mechanisms, etc. [4,5]. Although passive vibration control is a proven technique to reduce vibration transmission between vibration sources and receiving structures, conflicting requirements are often encountered in passive control applications and these can lead to limitations in control capabilities when the source and receiving structures are compliant and dynamical interactions between them exist [6,7].

Active control systems are capable of overcoming these limitations and allow performance enhancement and efficiency of vibration control [1,2,7–20]. Their applications range widely and include, for example, the reduction of ground excitation to vehicle passage; the elimination of transmitted vibrations in marine, aircraft and space structures; the prevention of machinery vibrations transmitting to surrounding environments; the vibration protection of sensitive equipment operating in harsh environments, to name but a few applications. The improvement of isolation effectiveness adopting active control strategies was undertaken by Jenkins et al. [7], who illustrated the potential for combined active/passive isolation schemes. Leo and Inman [8] developed a quadratic programming algorithm to study the design trade-offs of a one-degree-of-freedom single-axis active–passive vibration isolation system. Pare and How [9] proposed a hybrid feed-forward and feedback controller design approach to structural vibration control and developed a simple structural isolation example to demonstrate the benefit of an optimal hybrid controller to improve simultaneously isolation performance together with a reduction in closed-loop control bandwidth. Power flow and energy transfer approaches were examined to control, in an active manner, a vibration isolation system described by one- and two-degree-of-freedom dynamic models [10], in which fundamental concepts of active damping systems were studied by examining the average power flow in the controlled and passive actuators subject to harmonic inputs.

It is not unusual in studies of active vibration control [8–10] to adopt simplified models consisting of lumped elements or fixed base structures and to neglect the dynamic characteristics of flexible substructures and their interactions. Several authors [11–15] have assumed a flexible base, but treated the source structures as rigid bodies. Pan and Hansen [11] studied the dynamics of an active isolator by considering power transmission and thus extended the modelling of passive isolation systems in terms of power flow to the modelling of active isolators. They also applied this power flow control strategy to isolate vibrations from a rigid body to a plate through multiple mounts demonstrating the possibility of reducing power transmission to the plate. A study of active isolation from a rigid source structure through multiple mounts to a plate-like structure was presented in Ref. [12]. This flexible base rigid equipment (FBRE) isolation problem was also studied with the use of an active controller based on a linear quadratic Gaussian (LQG) control law [13]. To improve the isolation of mounted rigid equipment, characterized as a two-degree-of-freedom system, from base vibration Serrand and Elliott [14] investigated an

independent two-channel controller with absolute velocity feedback. More recently, this theory was extended by Kim et al. [15] using an impedance method to investigate a multichannel active vibration isolation system with four-mounts, including a decentralized velocity feedback control.

The rigid body simplification, introduced by neglecting the resonant effect of the source/receiver structure, is valid in low-frequency vibration control studies. However, it can lead to problems in the medium to high-frequency range particularly if the impedance of the source and receiving structure are comparable [6]. More recently, active control of complex dynamic systems with elastic structures has received attention. For example, for coupled flexible structures, Kaplow and Velman [16] isolated two structures by using active mounts to apply forces between the structures. Their characteristics were related to acceleration measurements permitting zero acceleration of the isolated structure. Scribner et al. [17] described an active isolation technique based on classical disturbance rejection ideas. The transmitted force is fed back to a single-degree-of-freedom mount through a classical compensator to provide rejection of the transmitted force and effective vibration isolation is achieved within a narrow frequency band. The force feedback method for active vibration isolation was studied by Clark and Robertshaw [18] who showed how a multiple-degree-of-freedom vibration isolation problem can be localized to the individual links of the adaptive components. Gardonio and Elliott [19] presented a mobility–impedance matrix model to predict vibration transmission between two plates connected by a number of active mounts and investigated three different active control strategies including the reduction of the total structural power transmission from source to receiver.

Many different types of mathematical models [7–19] have been developed to study coupled systems built of coupled rigid and/or flexible substructures and control systems. Each model examines in detail some chosen typical problem. It is surprising that investigation into the dynamics and energy transmission mechanisms of a generalized integrated structure–control system in which active control subsystems are retrofitted into a complex existing passive control system are few and far between, although progress has been made for simple one-degree-of-freedom systems by Gardonio and Elliott [19] and Margolis [20]. More complex cases relating to vehicle–bridge-control interaction systems and complex multi-dimensional flexible isolation systems are examined in Refs. [21–24]. Here two efficient progressive approaches are presented to analyze power flows in general dynamical systems consisting of any number of rigid/flexible substructures.

The modelling and design of an active control system consisting of flexible structures/components is of practical importance for technological developments in many engineering sectors. The fundamental barriers to progress and development of a comprehensive approach are found in the lack of good mathematical models to deal with general passive–active dynamical interaction systems and the difficulties to perform effectively the dynamic analysis in extensive, multi-dimensional complex coupled systems. This paper therefore attempts to develop a general analytical framework to overcome these barriers with the objectives of:

(i) to model generic complex structure–control synthesized systems composed of multiple substructures subject to general boundary conditions and multiple excitations. The system model consists of any number of three-dimensional rigid/flexible substructures and control subsystems with multiple channels;
(ii) to present an integrated framework to solve various vibration isolation and control problems including general passive, active, hybrid control problems as well as their dynamic

interactions, which provides a basis to develop a general computer program that may allow the user to build arbitrarily complex linear control models using simple commands and inputs;

(iii) to investigate general passive, active, hybrid control problems as well as their dynamic interaction to evaluate and improve their control effectiveness;

(iv) to describe the dynamical behaviour of the integrated structure–control system through receptance, transmissibility, mobility, transfer functions, etc.;

(v) to analyze the vibratory energy transmission mechanisms and to evaluate their magnitudes on coupling interfaces between interacting subsystems within the continuous/discontinuous substructures of the overall system.

2. Dynamics of generalized control structure composite system

2.1. System model

Consider N substructures $S^{(s)}$ $(s = 1, 2, \ldots, N)$ interconnected at multiple points by $n_I^{(s,t)}(t \in H^{(s)}, s \notin H^{(s)})$ passive-active control subsystems and constrained by $n_J^{(s,0)} + n_J^{(t,0)}$ sky-hook controller subsystems. Fig. 1 illustrates a representative substructure $S^{(s)}$ $(s = 1, 2, \ldots, N)$ coupled with substructures $S^{(t)}$ $(t \in H^{(s)}, s \notin H^{(s)})$ chosen from a generalized dynamical substructure–control interaction system consisting of N substructures under examination. Here $H^{(s)}$ represents a set of numbers identifying the substructures connected to substructure $S^{(s)}$. This system is a complicated hybrid system incorporating rigid/elastic structures and active/passive vibration controllers. It is well known that a hybrid control system is typically defined as one that employs a combination of passive and active devices. One assumes that all controllers are of zero mass compared with the masses of the substructures to be studied. To describe the dynamics of this system, a standard Cartesian tensor index ($i = 1, 2, 3$) and a summation convention are applied herein.

As schematically illustrated in Fig. 1, O-$X_1X_2X_3$ is a global Cartesian co-ordinate reference system fixed in the three-dimensional space describing the position of the integrated system, and the local co-ordinate system fixed at the point $o^{(s)}(X_1^{(s)}X_2^{(s)}X_3^{(s)})$ in/on substructure $S^{(s)}$ is denoted by $o^{(s)}$-$x_1^{(s)}x_2^{(s)}x_3^{(s)}$. The transformation tensor from local system $o^{(s)}$-$x_1^{(s)}x_2^{(s)}x_3^{(s)}$ to global co-ordinate system O-$X_1X_2X_3$ is represented by $\theta_{ij}^{(s)}$, where $\theta_{ij}^{(s)} = \cos(X_i \hat{} x_j^{(s)})$, i.e., the directional cosine of the angle between axis X_i and $x_j^{(s)}$. The typical substructure $S^{(s)}$ occupies a domain $V^{(s)}$ with the boundary $\Gamma^{(s)} = S_u^{(s)} \cup S_T^{(s)}$ having a unit vector $\mathbf{v}^{(s)}$ defined along its outer normal. Here $S_u^{(s)}$ and $S_T^{(s)}$ denote, respectively, the displacement boundary and the traction boundary, respectively. As the case shown in the figure, for $S^{(s)}$ there is no displacement boundary, i.e., $S_u^{(s)}$ is an empty set.

The substructure $S^{(s)}$ may represent an elastic machine or equipment or supporting structures of finite size with arbitrary configuration to which the generalized external excitation force vector $\mathbf{f}_i^{(s)} = \{f_{1i}^{(s)}, f_{2i}^{(s)}, \ldots, f_{Li}^{(s)}, \ldots, f_{n^{(s)}i}^{(s)}\}^{\mathrm{T}}$ applies with harmonic frequency Ω, where $f_{Li}^{(s)} = F_{Li}^{(s)} e^{j\Omega t}$ acting, respectively, at points $\mathbf{x}_L^{(s)}$ $(L = 1, 2, \ldots, n^{(s)})$. Denoting $\mathbf{F}_i^{(s)} = \{F_{1i}^{(s)}, F_{2i}^{(s)}, \ldots, F_{Li}^{(s)}, \ldots, F_{n^{(s)}i}^{(s)}\}^{\mathrm{T}}$, one has $\mathbf{f}_i^{(s)} = \mathbf{F}_i^{(s)} e^{j\Omega t}$. The substructure $S^{(s)}$ is coupled to substructures $S^{(t)}$ by the $n_I^{(s,t)} = n_I^{(t,s)}$ hybrid active–passive control systems. A typical Ith $(I = 1, 2, \ldots, n_I^{(s,t)})$ hybrid control system illustrated in Fig. 1 connects the two arbitrary chosen points $\mathbf{x}_I^{(s,t)} \in V^{(s)}$ and $\mathbf{x}_I^{(t,s)} \in V^{(t)}$. This control system

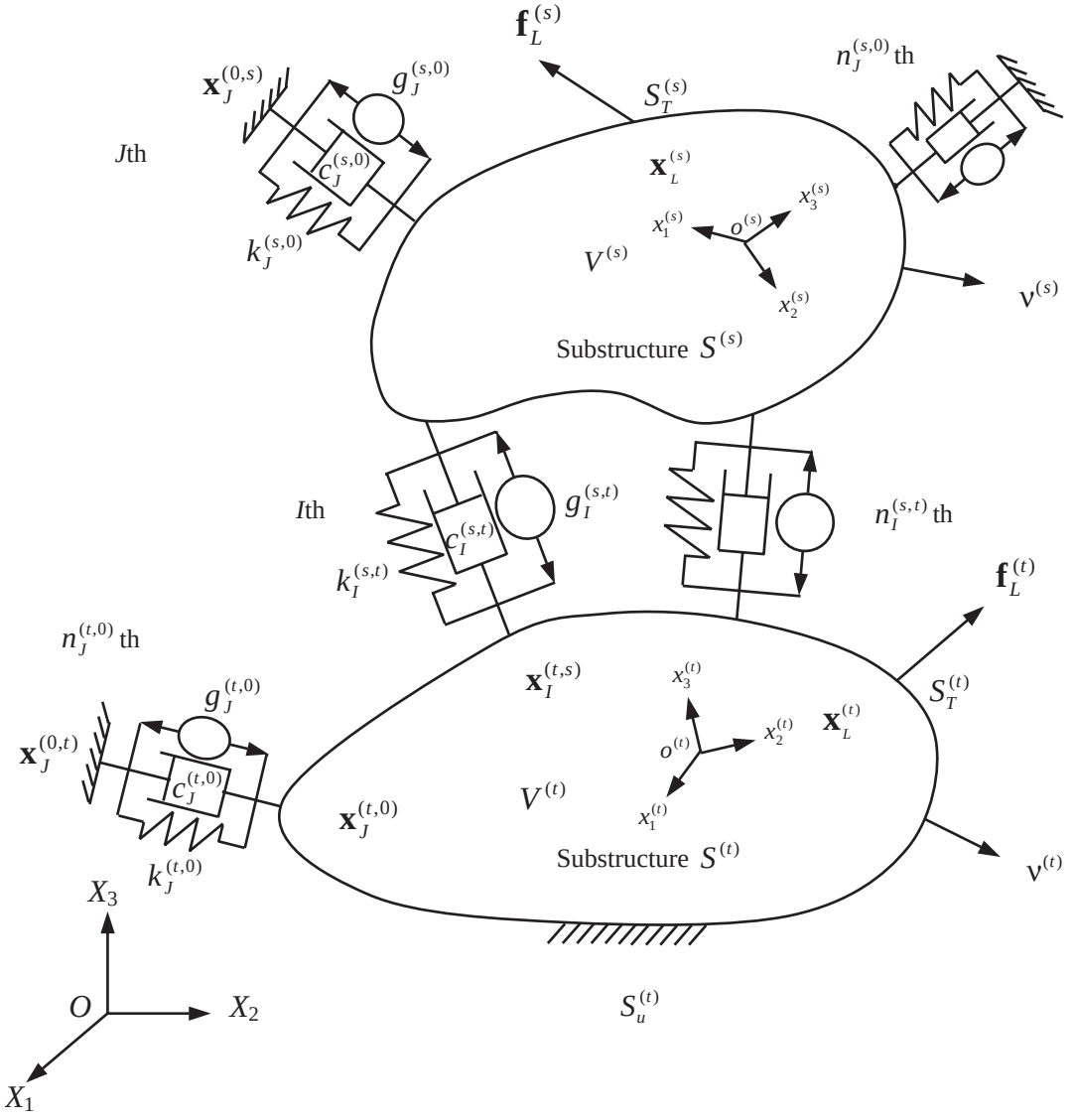

Fig. 1. A generalized hybrid active–passive vibration control model for interconnected three-dimensional flexible and/or rigid structures with multiple couplings of multiple-degree-of-freedom subject to multiple excitations.

consists of a spring of stiffness $k_I^{(s,t)} = k_I^{(t,s)}$, a damper of viscous damping coefficient $c_I^{(s,t)} = c_I^{(t,s)}$ and an active controller with its relative velocity feedback of gain $g_I^{(s,t)} = g_I^{(t,s)}$ produced by active control devices.

The $n_J^{(s,0)}$ sky-hook controllers are used to provide active–passive control forces associated with the absolute motion of the substructure $S^{(s)}$. A typical Jth ($J = 1, 2, \ldots, n_J^{(s,0)}$) sky-hook controller, fixed at the two points $\mathbf{x}_J^{(s,0)} \in V^{(s)}$ and $\mathbf{x}_J^{(0,s)}$ on the earth, consists of a spring of stiffness $k_J^{(s,0)}$, a damper of viscous damping coefficient $c_J^{(s,0)}$ and an absolute velocity feedback controller of gain $g_J^{(s,0)}$ produced by active control devices. In the model describing the active control system,

double-acting operating actuators are used as shown in the figure. If there is no sky-hook controllers applied to substructure $S^{(s)}$, then $n_J^{(s,0)} = 0$. The spatial orientation of all the integrated active–passive controllers are arbitrarily chosen and can be fully determined by their directional cosine vectors in terms of the end co-ordinates of the coupling points given by Eq. (6).

This general mathematical model covers a wide a range of dynamical systems and control models studied in the literature [7–20, 22, 23]. For example, in particular applications to vibration isolation problems, this general model is suitable to describe both types of isolation problems, i.e., (i) the isolation between the vibration source (machine/equipment) and the receiver when the excitation is caused by forces acting on the source structure, and (ii) the isolation between equipment and foundation when the excitation is caused by the motion of the foundation. The effects of sky-hook (or absolute velocity feedback) control subsystems are also addressed in the proposed model.

This generalized model allows study of passive, active and hybrid control strategies from an energy-based control viewpoint and transitional dynamic response or vibration transmissibility. It allows understanding of control mechanisms and the effectiveness of various control arrangements as well as determining the power flow characteristics of complex integrated systems consisting of either distributed or rigid substructures having general three-dimensional configurations. Furthermore, it is a convenient model to investigate the dynamical behaviour of a pre-existing passive control system retrofitted by an active control subsystem to assess control efficiency and/or control strategy of operation.

2.2. Governing equations

The material co-ordinate system of solid mechanics is adopted to describe the motion of substructures [25]. Let one assume that $u_i^{(s)}$ and $v_i^{(s)}$ represent the displacement and velocity of a typical substructure $S^{(s)}$, respectively, $\rho^{(s)}$ denotes the mass density of the continuum, $\sigma_{ij}^{(s)}$ the complex stress tensor, $\varepsilon_{ij}^{(s)}$ the strain tensor, and $\eta^{(s)}$ the loss modulus coefficients. Using this notation, the summation convention of tensor analysis and the fundamental equations and principles of continuum mechanics, allow the governing equations describing the coupling dynamics of the control system for the two continuum substructures $S^{(s)}$ shown in Fig. 1 to be written as

(i) *Dynamic equation*:

$$\sigma_{ij,j}^{(s)} = \rho^{(s)} u_{i,tt}^{(s)}, \quad \mathbf{x} \in V^{(s)}, \tag{1}$$

in which the gravitation force is neglected.

(ii) *Constitutive equation*: A hysteretic energy-absorption mechanism model is adopted and a complex modulus of elasticity, i.e., $E_{ijkl}^{*(s)} = E_{ijkl}^{(s)}(1 + \mathrm{j}\eta^{(s)})$ is introduced. Alternative models may be substituted for this hysterestic model but the general approach proposed remains with suitable modifications. The complex stress–strain tensor relation is represented as

$$\sigma_{ij}^{(s)} = E_{ijkl}^{*(s)} \varepsilon_{kl}^{(s)} = E_{ijkl}^{(s)}(1 + \mathrm{j}\eta^{(s)})\varepsilon_{kl}^{(s)}, \quad \mathbf{x} \in V^{(s)}. \tag{2}$$

(iii) *Strain–displacement relation*:

$$\varepsilon_{kl}^{(s)} = \tfrac{1}{2}(u_{k,l}^{(s)} + u_{l,k}^{(s)}), \quad \mathbf{x} \in V^{(s)}. \tag{3}$$

(iv) *Boundary condition*
traction:

$$\sigma_{ij}^{(s)}\nu_j^{(s)} = \sum_{L=1}^{n^{(s)}} f_{Li}^{(s)}\delta(\mathbf{x}-\mathbf{x}_L^{(s)}) + \sum_{t\in H^{(s)}}\sum_{I=1}^{n_I^{(s,t)}} f_I^{(s,t)}\delta(\mathbf{x}-\mathbf{x}_I^{(s,t)})\alpha_{Ii}^{(s,t)} + \sum_{J=1}^{n_I^{(s,0)}} f_J^{(s,0)}\delta(\mathbf{x}-\mathbf{x}_J^{(s,0)})\beta_{Ji}^{(s,0)},$$
$$\mathbf{x}\in S_T^{(s)}. \tag{4}$$

displacement:

$$u_i^{(s)} = 0, \quad \mathbf{x}\in S_u^{(s)}, \tag{5}$$

where $\alpha_{Ii}^{(s,t)}$ and $\beta_{Ji}^{(s,0)}$ represent the unit directional cosine vectors in the local co-ordinate system along which the Ith hybrid control subsystem and the Jth sky-hook controller are mounted, respectively. They are defined by

$$\alpha_{Ii}^{(s,t)} = \theta_{ij}^{(s)\mathrm{T}}\tilde{\alpha}_{Ij}^{(s,t)}, \quad \beta_{Ji}^{(s,0)} = \theta_{ij}^{(s)\mathrm{T}}\tilde{\beta}_{Ij}^{(s,0)}, \tag{6a, b}$$

where $\tilde{\alpha}_{Ii}^{(s,t)}$ and $\tilde{\beta}_{Ji}^{(s,0)}$ represent, respectively, the unit directional cosine vectors of the I*th* hybrid active–passive controller and J*th* sky hooker in the global co-ordinate system, i.e.,

$$\tilde{\alpha}_{Ii}^{(s,t)} = \frac{X_{Ii}^{(t,s)} - X_{Ii}^{(s,t)}}{\sqrt{(X_{Ij}^{(t,s)} - X_{Ij}^{(s,t)})(X_{Ij}^{(t,s)} - X_{Ij}^{(s,t)})}}, \tag{6c}$$

$$\tilde{\beta}_{Ji}^{(s,0)} = \frac{X_{Ji}^{(0,s)} - X_{Ji}^{(s,0)}}{\sqrt{(X_{Jj}^{(0,s)} - X_{Jj}^{(s,0)})(X_{Jj}^{(0,s)} - X_{Jj}^{(s,0)})}}, \tag{6d}$$

$$X_{Ii}^{(s,t)} = X_i^{(s)} + \theta_{ij}^{(s)}x_{Ij}^{(s,t)}, \quad X_{Ji}^{(s,t)} = X_i^{(s)} + \theta_{ij}^{(s)}x_{Ij}^{(s,t)} \quad (s = 1, 2, \ldots, N). \tag{6e}$$

With this definition, the positive direction of the unit directional cosine vector points outwards from substructure $S^{(s)}$.

The control force vectors take the forms

$$f_I^{(s,t)} = f_{pI}^{(s,t)} + f_{aI}^{(s,t)}, \quad f_J^{(s,0)} = f_{pJ}^{(s,0)} + f_{aJ}^{(s,0)}, \tag{7, 8}$$

where $f_{pI}^{(s,t)}$ denotes the Ith passive coupling force between the two substructures $S^{(s)}$ and $S^{(t)}$, $f_{aI}^{(s,t)}$ the Ith active control force associated with the Ith relative velocity feedback controller, and $f_{pJ}^{(s,0)}$,$f_{aJ}^{(s,0)}$ denote the Jth passive control force and active absolute control force applied to the substructure $S^{(s)}$ produced by the Jth sky-hook controller. These are calculated from the expressions

$$f_{pI}^{(s,t)} = -\tilde{\alpha}_{Ii}^{(s,t)}\{k_I^{(s,t)}[\theta_{ij}^{(s)}u_j^{(s)}(\mathbf{x}_I^{(s,t)}, t) - \theta_{ij}^{(t)}u_j^{(t)}(\mathbf{x}_I^{(t,s)}, t)] + c_I^{(s,t)}[\theta_{ij}^{(s)}\dot{u}_j^{(s)}(\mathbf{x}_I^{(s,t)}, t) - \theta_{ij}^{(t)}\dot{u}_j^{(t)}(\mathbf{x}_I^{(t,s)}, t)]\}, \tag{9}$$

$$f_{aI}^{(s,t)} = -g_I^{(s,t)}\tilde{\alpha}_{Ii}^{(s,t)}[\theta_{ij}^{(s)}\dot{u}_j^{(s)}(\mathbf{x}_I^{(s,t)}, t) - \theta_{ij}^{(t)}\dot{u}_j^{(t)}(\mathbf{x}_I^{(t,s)}, t)] \quad (I = 1, 2, \ldots, n^{(s,t)}), \tag{10}$$

$$f_{pJ}^{(s,0)} = -\tilde{\beta}_{Ji}^{(s,0)}[k_J^{(s,0)}\theta_{ij}^{(s)}u_j^{(s)}(\mathbf{x}_J^{(s,0)}, t) + c_J^{(s,0)}\theta_{ij}^{(s)}\dot{u}_j^{(s)}(\mathbf{x}_J^{(s,0)}, t)], \tag{11}$$

$$f_{aJ}^{(s,0)} = -g_J^{(s,0)}\tilde{\beta}_{Ji}^{(s,0)}\theta_{ij}^{(s)}\dot{u}_j^{(s)}(\mathbf{x}_J^{(s,0)}, t) \quad (J = 1, 2, \ldots, n^{(s,0)}). \tag{12}$$

2.3. Analytical solution

The analytical solution of the dynamic response of the complex coupled system described by the governing equations in Section 2.2 is derived as follows.

On substituting Eq. (3) into Eq. (2) and then into Eqs. (1) and (4), respectively, we obtain the results

$$E^{*(s)}_{ijkl}u^{(s)}_{k,lj} = \rho^{(s)}u^{(s)}_{i,tt}, \tag{13}$$

$$E^{*(s)}_{ijkl}u^{(s)}_{k,l}v^{(s)}_{j} = \sum_{L=1}^{n^{(s)}} f^{(s)}_{Li}\delta(\mathbf{x}-\mathbf{x}^{(s)}_{L}) + \sum_{t\in H^{(s)}}\sum_{I=1}^{n^{(s,t)}_{I}} f^{(s,t)}_{I}\delta(\mathbf{x}-\mathbf{x}^{(s,t)}_{I})\alpha^{(s,t)}_{Ii} + \sum_{J=1}^{n^{(s,0)}_{J}} f^{(s,0)}_{J}\delta(\mathbf{x}-\mathbf{x}^{(s,0)}_{J})\beta^{(s,0)}_{Ji}. \tag{14}$$

Based on the mode superposition method described by Thomson [4], the displacement field $u^{(s)}_{i}(\mathbf{x},t)$ of the elastic substructure $S^{(s)}$ can be expressed as a linear combination of the natural mode functions in terms of a mode shape vector matrix $\mathbf{\Phi}^{(s)}_{i}(\mathbf{x}) = [\varphi^{(s)}_{i1}, \varphi^{(s)}_{i2}, \ldots, \varphi^{(s)}_{iN^{(s)}}]$ represented in its local system and a generalized co-ordinate vector $\mathbf{q}^{(s)}(t) = [q_1, q_2, \ldots, q_{N^{(s)}}]^{(s)\mathrm{T}}$, where $N^{(s)}$ is the number of system modes admitted into the mathematical model. Here $\varphi^{(s)}_{in}$ $(n = 1, 2, \ldots, N^{(s)})$ represents the retained natural modes of substructures $S^{(s)}$, i.e., the vibration modes of the substructures $S^{(s)}$ with no damping and external loads (see Appendix A). It has been accepted that such combined dynamical systems are unlikely to have real-valued mode shapes if any damping is present [26]. In this paper, only the natural modes of a substructure are used as base vectors of the motion space to represent its vibration configuration, which is a widely adopted approach in vibration analysis [4,27].

The modal decomposition formulations for substructures $S^{(s)}$ take the following component forms:

$$u^{(s)}_{i}(\mathbf{x},t) = \mathbf{\Phi}^{(s)}_{i}(\mathbf{x})\mathbf{q}^{(s)}(t) = \mathbf{\Phi}^{(s)}_{i}(\mathbf{x})\mathbf{Q}^{(s)}\mathrm{e}^{\mathrm{j}\Omega t}, \quad \mathbf{x}\in V^{(s)}, \tag{15}$$

where

$$\mathbf{Q}^{(s)} = [Q^{(s)}_{1}, Q^{(s)}_{2}, \ldots, Q^{(s)}_{N^{(s)}}]^{\mathrm{T}}. \tag{16}$$

A substitution of Eq. (15) into Eqs. (13) and (14), as well as Eq. (5) gives

$$E^{*(s)}_{ijkl}\mathbf{\Phi}^{(s)}_{k,lj}\mathbf{Q}^{(s)} = -\rho^{(s)}\mathbf{\Phi}^{(s)}_{i}\mathbf{Q}^{(s)}\Omega^2, \tag{17}$$

$$\begin{aligned} E^{*(s)}_{ijkl}\mathbf{\Phi}^{(s)}_{k,l}\mathbf{Q}^{(s)}v^{(s)}_{j} = {} & \sum_{L=1}^{n^{(s)}} f^{(s)}_{Li}\delta(\mathbf{x}-\mathbf{x}^{(s)}_{L}) \\ & + \sum_{t\in H^{(s)}}\sum_{I=1}^{n^{(s,t)}_{I}} f^{(s,t)}_{I}\delta(\mathbf{x}-\mathbf{x}^{(s,t)}_{I})\alpha^{(s,t)}_{Ii} + \sum_{J=1}^{n^{(s,0)}_{J}} f^{(s,0)}_{J}\delta(\mathbf{x}-\mathbf{x}^{(s,0)}_{J})\beta^{(s,0)}_{Ji}, \quad \mathbf{x}\in S^{(s)}_{T} \end{aligned} \tag{18}$$

$$\mathbf{\Phi}^{(s)}_{i}\mathbf{Q}^{(s)} = \mathbf{0}, \quad \mathbf{x}\in S^{(s)}_{u}. \tag{19}$$

On pre-multiplying Eq. (17) by $\mathbf{\Phi}^{(s)^{\mathrm{T}}}_{i}$ and integrating over the volume $V^{(s)}$, it follows that

$$\int_{V^{(s)}} \mathbf{\Phi}^{(s)^{\mathrm{T}}}_{i} E^{*(s)}_{ijkl}\mathbf{\Phi}^{(s)}_{k,lj}\mathbf{Q}^{(s)}\ \mathrm{d}V = -\int_{V^{(s)}} \rho^{(s)}\mathbf{\Phi}^{(s)^{\mathrm{T}}}_{i}\mathbf{\Phi}^{(s)}_{i}\mathbf{Q}^{(s)}\Omega^2\ \mathrm{d}V. \tag{20}$$

By using the Green theorem and the boundary condition (18), the left side integral of Eq. (20) becomes

$$\begin{aligned}
&\int_{V^{(s)}} \left\{ [\boldsymbol{\Phi}_i^{(s)\mathrm{T}} E_{ijkl}^{*(s)} \boldsymbol{\Phi}_{k,l}^{(s)} \mathbf{Q}^{(s)}]_{,\,j} - \boldsymbol{\Phi}_{i,j}^{(s)\mathrm{T}} E_{ijkl}^{*(s)} \boldsymbol{\Phi}_{k,l}^{(s)} \mathbf{Q}^{(s)} \right\} \mathrm{d}V \\
&\quad = \int_{S^{(s)}} \boldsymbol{\Phi}_i^{(s)\mathrm{T}} E_{ijkl}^{*(s)} \boldsymbol{\Phi}_{k,l}^{(s)} \mathbf{Q}^{(s)} v_j^{(s)} \,\mathrm{d}S - \int_{V^{(s)}} \boldsymbol{\Phi}_{i,j}^{(s)\mathrm{T}} E_{ijkl}^{*(s)} \boldsymbol{\Phi}_{k,l}^{(s)} \mathbf{Q}^{(s)} \,\mathrm{d}V \\
&\quad = \int_{S^{(s)}} \boldsymbol{\Phi}_i^{(s)\mathrm{T}} \left\{ \sum_{L=1}^{n^{(s)}} f_{Li}^{(s)} \delta(\mathbf{x} - \mathbf{x}_L^{(s)}) + \sum_{t \in H^{(s)}} \sum_{I=1}^{n_I^{(s,t)}} f_I^{(s,t)} \delta(\mathbf{x} - \mathbf{x}_I^{(s,t)}) \alpha_{Ii}^{(s,t)} + \sum_{J=1}^{n_J^{(s,0)}} f_J^{(s,0)} \delta(\mathbf{x} - \mathbf{x}_J^{(s,0)}) \beta_{Ji}^{(s,0)} \right\} \mathrm{d}S \\
&\qquad - \int_{V^{(s)}} \boldsymbol{\Phi}_{i,j}^{(s)\mathrm{T}} E_{ijkl}^{*(s)} \boldsymbol{\Phi}_{k,l}^{(s)} \mathbf{Q}^{(s)} \,\mathrm{d}V \\
&\quad = \sum_{L=1}^{n^{(s)}} \boldsymbol{\Phi}_i^{(s)\mathrm{T}}(\mathbf{x}_L^{(s)}) f_{Li}^{(s)} + \sum_{t \in H^{(s)}} \sum_{I=1}^{n_I^{(s,t)}} \boldsymbol{\Phi}_i^{(s)\mathrm{T}}(\mathbf{x}_I^{(s,t)}) f_I^{(s,t)} \alpha_{Ii}^{(s,t)} + \sum_{J=1}^{n_J^{(s,0)}} \boldsymbol{\Phi}_i^{(s)\mathrm{T}}(\mathbf{x}_J^{(s,0)}) f_J^{(s,0)} \beta_{Ji}^{(s,0)} \\
&\qquad - (1 + \mathrm{j}\eta^{(s)}) \mathbf{K}^{(s)} \mathbf{Q}^{(s)}
\end{aligned} \tag{21}$$

and the right side integral of Eq. (20) takes the form $-\Omega^2 \mathbf{M}^{(s)} \mathbf{Q}^{(s)}$, where

$$\mathbf{M}^{(s)} = \int_{V^{(s)}} \boldsymbol{\Phi}_i^{(s)\mathrm{T}} \rho^{(s)} \boldsymbol{\Phi}_i^{(s)} \,\mathrm{d}V, \quad \mathbf{K}^{(s)} = \int_{V^{(s)}} \boldsymbol{\Phi}_{i,j}^{(s)\mathrm{T}} E_{ijkl}^{(s)} \boldsymbol{\Phi}_{k,l}^{(s)} \,\mathrm{d}V = (\boldsymbol{\omega}^{(s)})^2 \mathbf{M}^{(s)}. \tag{22, 23}$$

Since the system is assumed linear, the eigenfunctions satisfy orthogonality properties (see Appendix A), and hence the matrices $\mathbf{M}^{(s)}$, $\mathbf{K}^{(s)}$ and $\boldsymbol{\omega}^{(s)}$ are of diagonal form. Therefore, Eq. (20) for substructure $S^{(s)}$ becomes

$$\begin{aligned}
&[(1 + \mathrm{j}\eta^{(s)})(\boldsymbol{\omega}^{(s)})^2 - \Omega^2 \mathbf{I}] \, \mathbf{M}^{(s)} \mathbf{Q}^{(s)} \\
&\quad = \sum_{L=1}^{n^{(s)}} \boldsymbol{\Phi}_i^{(s)\mathrm{T}}(\mathbf{x}_L^{(s)}) f_{Li}^{(s)} + \sum_{t \in H^{(s)}} \sum_{I=1}^{n_I^{(s,t)}} \boldsymbol{\Phi}_i^{(s)\mathrm{T}}(\mathbf{x}_I^{(s,t)}) f_I^{(s,t)} \alpha_{Ii}^{(s,t)} + \sum_{J=1}^{n_J^{(s,0)}} \boldsymbol{\Phi}_i^{(s)\mathrm{T}}(\mathbf{x}_J^{(s,0)}) f_J^{(s,0)} \beta_{Ji}^{(s,0)}.
\end{aligned} \tag{24}$$

Let one assume that the external forces are harmonic represented by the complex expression $\mathrm{e}^{\mathrm{j}\Omega t}$. The active–passive control forces in the direction of controllers have the same frequency Ω because the system is linear and from Eq. (7) can be represented by

$$f_I^{(s,t)} = F_I^{(s,t)} \mathrm{e}^{\mathrm{j}\Omega t}, \quad (I = 1, 2, \ldots, n_I^{(s,t)}), \tag{25}$$

where the complex amplitude $F_I^{(s,t)}$ derived from Eqs. (7), (9), (10) and (15) takes the form

$$F_I^{(s,t)} = -[k_I^{(s,t)} + \mathrm{j}\Omega(c_I^{(s,t)} + g_I^{(s,t)})] \alpha_{Ii}^{(s,t)} [\boldsymbol{\Phi}_i^{(s)}(\mathbf{x}_I^{(s,t)}) \mathbf{Q}^{(s)} - \boldsymbol{\Phi}_i^{(t)}(\mathbf{x}_I^{(t,s)}) \mathbf{Q}^{(t)}]. \tag{26}$$

Similarly, the active control forces produced by the sky-hook controllers and applied to the substructure $S^{(s)}$ $(s = 1, 2)$ are represented as

$$f_J^{(s,0)} = F_J^{(s,0)} \mathrm{e}^{\mathrm{j}\Omega t}, \quad (J = 1, 2, \ldots, n_J^{(s,0)}), \tag{27}$$

where

$$F_J^{(s,0)} = -[k_J^{(s,0)} + \mathrm{j}\Omega(c_J^{(s,0)} + g_J^{(s,0)})] \beta_{Ji}^{(s,0)} \boldsymbol{\Phi}_i^{(s)}(\mathbf{x}_J^{(s,0)}) \mathbf{Q}^{(s)} \tag{28}$$

The substitution of Eqs. (25)–(28) into Eq. (24) produces the final dynamic equations describing the characteristics of the coupled system. That is,

$$[(1+\mathrm{j}\eta^{(s)})(\boldsymbol{\omega}^{(s)})^2-\Omega^2\mathbf{I}]\mathbf{M}^{(s)}\mathbf{Q}^{(s)}=\sum_{L=1}^{n^{(s)}}\boldsymbol{\Phi}_i^{(s)^{\mathrm{T}}}(\mathbf{x}_L^{(s)})F_{Li}^{(s)}$$
$$-\sum_{t\in H^{(s)}}\sum_{I=1}^{n_I^{(s,t)}}\boldsymbol{\Phi}_i^{(s)^{\mathrm{T}}}(\mathbf{x}_I^{(s,t)})\alpha_{Ii}^{(s,t)}[k_I^{(s,t)}+\mathrm{j}\Omega(c_I^{(s,t)}+g_I^{(s,t)})]\alpha_{Il}^{(s,t)}[\boldsymbol{\Phi}_l^{(s)}(\mathbf{x}_I^{(s,t)})\mathbf{Q}^{(s)}-\boldsymbol{\Phi}_l^{(t)}(\mathbf{x}_I^{(t,s)})\mathbf{Q}^{(t)}]$$
$$-\sum_{J=1}^{n_J^{(s,0)}}\boldsymbol{\Phi}_i^{(s)^{\mathrm{T}}}(\mathbf{x}_J^{(s,0)})\beta_{Ji}^{(s,0)}[k_J^{(s,0)}+\mathrm{j}\Omega(c_J^{(s,0)}+g_J^{(s,0)})]\beta_{Jl}^{(s,0)}\boldsymbol{\Phi}_l^{(s)}(\mathbf{x}_J^{(s,0)})\mathbf{Q}^{(s)}. \tag{29}$$

or in matrix form

$$\mathbf{A}^{(s,s)}\mathbf{Q}^{(s)}+\sum_{t\in H^{(s)}}\mathbf{A}^{(s,t)}\mathbf{Q}^{(t)}=\mathbf{F}^{(s)}, \tag{30}$$

where

$$\mathbf{F}^{(s)}=\sum_{L=1}^{n^{(s)}}\boldsymbol{\Phi}_i^{(s)^{\mathrm{T}}}(\mathbf{x}_L^{(s)})F_{Li}^{(s)}=\mathbf{B}_i^{(s)}\mathbf{F}_i^{(s)}, \tag{31}$$

$$\mathbf{A}^{(s,s)}=[(1+\mathrm{j}\eta^{(s)})(\boldsymbol{\omega}^{(s)})^2-\Omega^2\mathbf{I}]\ \mathbf{M}^{(s)}+\mathbf{G}^{(s)}, \tag{32}$$

$$\mathbf{A}^{(s,t)}=-\sum_{I=1}^{n_I^{(s,t)}}\boldsymbol{\Phi}_i^{(s)^{\mathrm{T}}}(\mathbf{x}_I^{(s,t)})\alpha_{Ii}^{(s,t)}[k_I^{(s,t)}+\mathrm{j}\Omega(c_I^{(s,t)}+g_I^{(s,t)})]\alpha_{Il}^{(s,t)}\boldsymbol{\Phi}_l^{(t)}(\mathbf{x}_I^{(t,s)}), \tag{33}$$

$$\mathbf{G}^{(s)}=\sum_{t\in H^{(s)}}\sum_{I=1}^{n_I^{(s,t)}}\boldsymbol{\Phi}_i^{(s)^{\mathrm{T}}}(\mathbf{x}_I^{(s,t)})\alpha_{Ii}^{(s,t)}[k_I^{(s,t)}+\mathrm{j}\Omega(c_I^{(s,t)}+g_I^{(s,t)})]\alpha_{Il}^{(s,t)}\boldsymbol{\Phi}_l^{(s)}(\mathbf{x}_I^{(s,t)}),$$
$$+\sum_{J=1}^{n_J^{(s,0)}}\boldsymbol{\Phi}_i^{(s)^{\mathrm{T}}}(\mathbf{x}_J^{(s,0)})\beta_{Ji}^{(s,0)}[k_J^{(s,0)}+\mathrm{j}\Omega(c_J^{(s,0)}+g_J^{(s,0)})]\beta_{Jl}^{(s,0)}\boldsymbol{\Phi}_l^{(s)}(\mathbf{x}_J^{(s,0)}). \tag{34}$$

Obviously, if a substructure $S^{(r)}$ is not connected to substructure $S^{(s)}$, i.e., $r\notin H^{(s)}$, then $\mathbf{A}^{(s,r)}=\mathbf{0}$. The matrices $\mathbf{B}_i^{(s)}$ are transformation matrices of orders $(N^{(s)}\times n^{(s)})$ between the physical excitation forces and the generalized forces in the modal domain, respectively. They take the forms

$$\mathbf{B}_i^{(s)}=[\boldsymbol{\Phi}_i^{(s)^{\mathrm{T}}}(\mathbf{x}_1^{(s)}),\boldsymbol{\Phi}_i^{(s)^{\mathrm{T}}}(\mathbf{x}_2^{(s)}),\ldots,\boldsymbol{\Phi}_i^{(s)^{\mathrm{T}}}(\mathbf{x}_{n^{(s)}}^{(s)})]$$
$$=\begin{bmatrix}\varphi_{i1}^{(s)}(\mathbf{x}_1^{(s)}) & \varphi_{i1}^{(s)}(\mathbf{x}_2^{(s)}) & \cdots & \varphi_{i1}^{(s)}(\mathbf{x}_{n^{(s)}}^{(s)})\\ \varphi_{i2}^{(s)}(\mathbf{x}_1^{(s)}) & \varphi_{i2}^{(s)}(\mathbf{x}_2^{(s)}) & \cdots & \varphi_{i2}^{(s)}(\mathbf{x}_{n^{(s)}}^{(s)})\\ \vdots & \vdots & \ddots & \vdots\\ \varphi_{iN^{(s)}}^{(s)}(\mathbf{x}_1^{(s)}) & \varphi_{iN^{(s)}}^{(s)}(\mathbf{x}_2^{(s)}) & \cdots & \varphi_{iN^{(s)}}^{(s)}(\mathbf{x}_{n^{(s)}}^{(s)})\end{bmatrix}_{N^{(s)}\times n^{(s)}}. \tag{35}$$

In considering the whole system consisting of N substructures, Eq. (30) is extended to

$$\begin{bmatrix} \mathbf{A}^{(1,1)} & \mathbf{A}^{(1,2)} & \cdots & \mathbf{A}^{(1,N)} \\ \mathbf{A}^{(2,1)} & \mathbf{A}^{(2,2)} & \cdots & \mathbf{A}^{(2,N)} \\ \vdots & \vdots & \ddots & \vdots \\ \mathbf{A}^{(N,1)} & \mathbf{A}^{(N,2)} & \cdots & \mathbf{A}^{(N,N)} \end{bmatrix} \begin{Bmatrix} \mathbf{Q}^{(1)} \\ \mathbf{Q}^{(2)} \\ \vdots \\ \mathbf{Q}^{(N)} \end{Bmatrix} = \begin{Bmatrix} \mathbf{F}^{(1)} \\ \mathbf{F}^{(2)} \\ \vdots \\ \mathbf{F}^{(N)} \end{Bmatrix}. \tag{36}$$

This is a set of linear algebraic equations from which the unknown generalized co-ordinate vectors $\mathbf{Q}^{(s)}$ $(s = 1, 2, \ldots, N)$ can be determined.

For the case of a system consisting of two substructures, i.e., $N = 2$, the solution of Eq. (36) can be obtained in a simple analytical form as follows:

$$\begin{bmatrix} \mathbf{A}^{(11)} & \mathbf{A}^{(12)} \\ \mathbf{A}^{(21)} & \mathbf{A}^{(22)} \end{bmatrix}^{-1} = \begin{bmatrix} \mathbf{C}^{(11)} & \mathbf{C}^{(12)} \\ \mathbf{C}^{(21)} & \mathbf{C}^{(22)} \end{bmatrix}, \tag{37}$$

where

$$\begin{aligned} &\mathbf{C}^{(22)} = [\mathbf{A}^{(22)} - \mathbf{A}^{(21)}(\mathbf{A}^{(11)})^{-1}\mathbf{A}^{(12)}]^{-1}, \quad \mathbf{C}^{(12)} = -(\mathbf{A}^{(11)})^{-1}\mathbf{A}^{(12)}\mathbf{C}^{(22)}, \\ &\mathbf{C}^{(21)} = -\mathbf{C}^{(22)}\mathbf{A}^{(21)}(\mathbf{A}^{(11)})^{-1}, \quad \mathbf{C}^{(11)} = (\mathbf{A}^{(11)})^{-1} - \mathbf{C}^{(12)}\mathbf{A}^{(21)}(\mathbf{A}^{(11)})^{-1}, \end{aligned} \tag{38}$$

and therefore

$$\mathbf{Q}^{(s)} = \mathbf{C}^{(ss)}\mathbf{F}^{(s)} + \mathbf{C}^{(st)}\mathbf{F}^{(t)} \quad (s, t = 1, 2, s \neq t). \tag{39}$$

For the general system composed of any number of substructures $S^{(s)}$ $(s = 1, 2, \ldots, N)$ as shown in Fig. 1, the displacement and velocity response vectors of substructure $S^{(s)}$ are finally obtained from Eqs. (15), (16) and (36) in the local system as

$$u_i^{(s)}(\mathbf{x}, t) = \mathbf{\Phi}_i^{(s)}(\mathbf{x})\mathbf{q}^{(s)}(t) = \mathbf{\Phi}_i^{(s)}(\mathbf{x})\mathbf{Q}^{(s)}\mathrm{e}^{\mathrm{j}\Omega t}, \tag{40}$$

$$v_i^{(s)}(\mathbf{x}, t) = \dot{u}_i^{(s)}(\mathbf{x}, t) = \mathbf{\Phi}_i^{(s)}(\mathbf{x})\dot{\mathbf{q}}^{(s)}(t) = \mathrm{j}\Omega u_i^{(s)}(\mathbf{x}, t). \tag{41}$$

The coupling forces used to predict the vibratory power transmitted among substructures can be obtained from Eqs. (25)–(28).

3. Power flow analysis

3.1. Power flow formulations

3.1.1. Instantaneous power flow

In dynamical analyses, harmonic quantities are often represented mathematically by real harmonic functions. For example, a real harmonic force $f(t)$ with amplitude F and frequency ω, or a real velocity $v(t)$ with amplitude V, frequency ω and relative phase angle θ, are written in the forms $f(t) = F\cos\omega t$ and $v(t) = V\cos(\omega t + \theta)$. Alternatively, in complex mathematical notations, these quantities can be expressed as $\tilde{f}(t) = F\mathrm{e}^{\mathrm{j}\omega t}$ and $\tilde{v}(t) = V\mathrm{e}^{\mathrm{j}(\omega t+\theta)}$. In these expressions, the superscript tilde denotes a complex quantity. In this paper, the real part of the complex quantity is chosen to represent the corresponding physical quantity such that the force

$f(t) = \mathrm{Re}\{\tilde{f}(t)\}$ and the velocity $v(t) = \mathrm{Re}\{\tilde{v}(t)\}$. For convenience, the superscript tilde is neglected in the following equations.

In a power flow analysis, the power is defined as the rate at which work is done and therefore it is a practical, measurable quantity. Thus, mathematically, the instantaneous power at time t is defined as

$$p = \mathrm{Re}\{f(t)\}\mathrm{Re}\{v(t)\}, \tag{42}$$

where $f(t)$ and $v(t)$ are the instantaneous values of the force and velocity at a point.

3.1.2. Time-averaged power flow

For a vibrating structure, the time-averaged vibrational power flow is a more descriptive parameter of the dynamical system than its instantaneous value. For a harmonic motion with frequency ω, the time average of the real power over a period of vibration $2\pi/\omega$, i.e., the mean power, is given by

$$P = \frac{\omega}{2\pi}\int_0^{2\pi/\omega} \mathrm{Re}\{f(t)\}\mathrm{Re}\{v(t)\}\ \mathrm{d}t, \tag{43}$$

which can be further expressed by the form [28]

$$P = \tfrac{1}{2}\mathrm{Re}\{f(t)v^*(t)\} = \tfrac{1}{2}\mathrm{Re}\{f^*(t)v(t)\}, \tag{44}$$

where the superscript * denotes the complex conjugate of the associated complex quantities.

3.1.3. Energy flow density vector

The concept of energy flow density vector developed by Xing and Price [29] allows modelling of power flow characteristics transmitted or exchanged within a continuum. This energy flow density vector is defined by the dot product of the real velocity v_j and real stress tensor σ_{ji} as expressed by

$$p_i = -\mathrm{Re}\{v_j\}\mathrm{Re}\{\sigma_{ji}\}, \tag{45}$$

which is a vector field function dependent on the co-ordinate x_j and time t, describing the power flow transmitted from one part to another in the distributed dynamical system. It allows the determination of the rate of power flow at each point in or on the continuum through a unit area having an outward pointing unit vector v_j by the equation

$$p_v = p_i v_i = -\mathrm{Re}\{v_j\}\mathrm{Re}\{\sigma_{ji}\}v_i = -\mathrm{Re}\{v_j\}\mathrm{Re}\{T_j\}. \tag{46}$$

Here $T_j = \sigma_{ji}v_i$ expresses the traction force on this unit area.

Physically, the ith component p_i of the energy flow density vector represents the summation of the individual power contributed by the three stress components σ_{1i}, σ_{2i} and σ_{3i} acting on the unit area, which has a normal along the ith direction of the co-ordinate system. A positive value of p_v represents the power flowing per unit time through the unit area along its outward normal v_i and, in a closed domain, a positive power represents the energy flow transmitted from inside to outside of the domain.

3.1.4. Energy flow balance equations

An application of the general theory developed in Ref. [29] produces the equations of energy-flow balance for substructure $S^{(s)}$ as follows:

$$\int_{S^{(s)}} p_v^{(s)}\,\mathrm{d}S = -\int_{V^{(s)}} [\dot{K}^{(s)} + \dot{\Pi}^{(s)}]\,\mathrm{d}V - \int_{V^{(s)}} \dot{D}^{(s)}\,\mathrm{d}V, \tag{47}$$

where

$$\dot{K}^{(s)} = \rho\ \mathrm{Re}\{v_i^{(s)}\}\mathrm{Re}\{\dot{v}_i^{(s)}\}, \tag{48a}$$

$$\dot{\Pi}^{(s)} = E_{ijkl}^{(s)}\mathrm{Re}\{\varepsilon_{ij}^{(s)}\}\mathrm{Re}\{\dot{\varepsilon}_{kl}^{(s)}\}, \tag{48b}$$

$$\dot{D}^{(s)} = (\eta^{(s)}/\Omega)E_{ijkl}^{(s)}\mathrm{Re}\{\dot{\varepsilon}_{ij}^{(s)}\}\mathrm{Re}\{\dot{\varepsilon}_{kl}^{(s)}\}. \tag{48c}$$

These terms represent, respectively, the rates of changes of the kinetic-energy, the strain-energy density and the energy absorbed by the damping per unit volume of the material of the substructures.

The time-averaged equation describing the energy-flow balance of the two substructures is

$$\int_{S^{(s)}} p_v^{(s)}\,\mathrm{d}S = -\int_{V^{(s)}} \eta^{(s)}\Omega\bar{\Pi}^{(s)}\,\mathrm{d}V, \tag{49}$$

where

$$\bar{\Pi}^{(s)} = \tfrac{1}{2}E_{ijkl}^{(s)}\bar{\varepsilon}_{ij}^{(s)}\bar{\varepsilon}_{kl}^{(s)}, \tag{50}$$

and the over bar on the strain tensor denotes the maximum value of the sinusoidal quantity. For harmonic motion, the kinetic energy and the strain energy remain unchanged after every cycle. It therefore follows that the time averages of the rates of change of these quantities and the mechanical energy density are all zero.

3.2. Input power generated by external forces

The vibration energy input generated by the external excitation source to the system can be characterized by the input power flow at the driving point of the excitation force. Following the definition of a positive value of the power $p_v^{(s)}$ given in Eq. (46), the input power flow for a system has a negative value. In consideration of this, an application of the power flow Eq. (42) gives the Lth instantaneous input power flow $p_{L,in}^{(s)}$ supplied by an external concentrated excitation force $f_{Li}^{(s)}$ at the input point $\mathbf{x}_L^{(s)}$ $(L = 1, 2, \ldots, n^{(s)})$ on the boundary $S_T^{(s)}$ of substructure $S^{(s)}$ in the form

$$\begin{aligned} p_{L,in}^{(s)} &= -\mathrm{Re}\{v_i^{(s)}(\mathbf{x}_L^{(s)})\}\mathrm{Re}\{f_{Li}^{(s)}\} = -\mathrm{Re}\{v_i^{(s)}(\mathbf{x}_L^{(s)})\}F_{Li}^{(s)}\cos(\Omega t) \\ &= -\mathrm{Re}\{\mathrm{j}\Omega\boldsymbol{\Phi}_i^{(s)}(\mathbf{x}_L^{(s)})\mathbf{Q}^{(s)}\mathrm{e}^{\mathrm{j}\Omega t}\}F_{Li}^{(s)}\cos(\Omega t) \quad (L = 1, 2, \ldots, n^{(s)}, \quad s = 1, 2, \ldots, N). \end{aligned} \tag{51a}$$

Hence, the total instantaneous external energy flow entering the substructure $S^{(s)}$, i.e., input power $p_{in}^{(s)}$ is

$$p_{in}^{(s)} = \sum_{L=1}^{n^{(s)}} p_{L,in}^{(s)}. \tag{51b}$$

Furthermore, from Eq. (44), it follows that the time-averaged input power $P_{L,in}^{(s)}$ of substructure $S^{(s)}$ by the Lth external concentrated excitation force is expressed as

$$P_{L,in}^{(s)} = -\tfrac{1}{2}\mathrm{Re}\{f_{Li}^{(s)} v_i^{*(s)}(\mathbf{x}_L^{(s)})\} = -\tfrac{1}{2}\mathrm{Re}\{f_{Li}^{*(s)} v_i^{(s)}(\mathbf{x}_L^{(s)})\}, \tag{52a}$$

and the total time-averaged input power $P_{in}^{(s)}$ injected by all the external concentrated excitation forces is given by

$$P_{in}^{(s)} = \sum_{L=1}^{n^{(s)}} P_{L,in}^{(s)}. \tag{52b}$$

3.3. Power flow transmission

3.3.1. Power flow transmission within substructures

The transmission of power flow within substructures can be described by the energy flow density vector. Based on Eq. (45), the energy flow density vector at any point on/in substructures $S^{(s)}$ in the local system is

$$p_i^{(s)} = -\mathrm{Re}\{v_j^{(s)}\}\mathrm{Re}\{\sigma_{ji}^{(s)}\} = -\mathrm{Re}\{\dot{u}_j^{(s)}\}\mathrm{Re}\{E_{ijkl}^{*(s)} u_{k,l}^{(s)}\}, \tag{53}$$

where the velocity vectors at any point $\mathbf{x} \in V^{(s)}$ of substructure $S^{(s)}$ in the coupled system are given by Eq. (40). A displacement gradient is derived by taking the derivative with respect to x_l of a displacement response given in Eq. (39). That is

$$u_{k,l}^{(s)} = \boldsymbol{\Phi}_{k,l}^{(s)}(\mathbf{x})\mathbf{q}^{(s)}(t) = \boldsymbol{\Phi}_{k,l}^{(s)}(\mathbf{x})\mathbf{Q}^{(s)} e^{j\Omega t}, \quad \mathbf{x} \in V^{(s)}. \tag{54}$$

The substitution of Eq. (54) into Eq. (53) yields

$$p_i^{(s)} = -\mathrm{Re}\{\dot{u}_j^{(s)}\}\mathrm{Re}\{E_{ijkl}^{*(s)} \boldsymbol{\Phi}_{k,l}^{(s)}(\mathbf{x})\mathbf{Q}^{(s)} e^{j\Omega t}\}, \quad \mathbf{x} \in V^{(s)}, \tag{55}$$

which determines the energy flow density vectors describing energy transmission between one part of the structure and another.

3.3.2. Power flow transmission between substructures

As shown in Fig. 1, the complex integrated structure-control dynamical system consists of N substructures $S^{(s)}, n_J^{(s,0)}$ absolute velocity feedback controllers and $n_I^{(s,t)}$ relative velocity feedback controllers. The power flow transmission between substructures $S^{(s)}$ and through the controllers is described by the power flows at their coupling points, which are calculated as follows.

For the Ith ($I = 1, 2, \ldots, n_I^{(s,t)}$) controller connecting the two points $\mathbf{x}_I^{(s,t)}$ of $S^{(s)}$ and $\mathbf{x}_I^{(t,s)}$ of $S^{(t)}$, it follows from Eq. (46) that the instantaneous output power $p_I^{(s,t)}$ at $\mathbf{x}_I^{(s,t)}$ from $S^{(s)}$ transmitting to $S^{(t)}$ is expressed as

$$p_I^{(s,t)} = \mathrm{Re}\{v_{Ii}^{(s)}(\mathbf{x}_I^{(s,t)})\alpha_{Ii}^{(s,t)}\}\mathrm{Re}\{f_I^{(s,t)}\} = \mathrm{Re}\{v_I^{(s)}(\mathbf{x}_I^{(s,t)})\}\mathrm{Re}\{f_I^{(s,t)}\}, \tag{56}$$

where $v_I^{(s)}(\mathbf{x}_I^{(s,t)}) = v_{Ii}^{(s)}(\mathbf{x}_I^{(s,t)})\alpha_{Ii}^{(s,t)}$ ($t \in H^{(s)}$) represents the velocity along the controller direction $\alpha_{Ii}^{(s,t)}$ at the point $\mathbf{x}_I^{(s,t)}$. The total instantaneous output power $p^{(s)}$ from $S^{(s)}$ through all the $n_I^{(s,t)}$

controllers is described by the form

$$p^{(s)} = \sum_{t \in H^{(s)}} \sum_{I=1}^{n_I^{(s,t)}} p_I^{(s,t)}. \tag{57}$$

The time-averaged and total power flow corresponding to $p_I^{(s,t)}$ and $p^{(s)}$ (i.e., $P_I^{(s,t)}$, $P^{(s)}$) are given, respectively, by

$$P_I^{(s,t)} = \tfrac{1}{2}\mathrm{Re}\{f_I^{(s,t)} v_I^{*(s)}(\mathbf{x}_I^{(s)})\}, \quad (I = 1, 2, \ldots, n_I^{(s,t)}), \tag{58}$$

$$P^{(s)} = \sum_{t \in H^{(s)}} \sum_{I=1}^{n_I^{(s,t)}} P_I^{(s)}. \tag{59}$$

For the Jth ($J = 1, 2, \ldots, n_J^{(s,0)}$) sky-hook controller mounted at point $x_J^{(0,s)}$ to a fixed position and the point $x_J^{(s,0)}$ on substructure $S^{(s)}$, the instantaneous output power $p_J^{(s,0)}$ at the point $x_J^{(s,0)}$, is described by

$$p_J^{(s,0)} = -\mathrm{Re}\{v_{Ji}^{(s)}(\mathbf{x}_J^{(s,0)})\beta_{Ji}^{(s,0)}\}\mathrm{Re}\{f_J^{(s,0)}\} = -\mathrm{Re}\{v_J^{(s)}(\mathbf{x}_J^{(s,0)})\}\mathrm{Re}\{f_J^{(s,0)}\}, \tag{60}$$

where $v_J^{(s)}(\mathbf{x}_J^{(s,0)}) = v_{Ji}^{(s)}(\mathbf{x}_J^{(s,0)})\beta_{Ji}^{(s,0)}$ denotes the velocity at the point $\mathbf{x}_J^{(s,0)}$ along the direction $\beta_{Ji}^{(s,0)}$ of the sky-hook controller. Hence, the total instantaneous output power $p_a^{(s)}$ from $S^{(s)}$ to all the $n_J^{(s,0)}$ sky-hook controllers is given by

$$p_a^{(s)} = \sum_{J=1}^{n_J^{(s,0)}} p_J^{(s,0)} = -\sum_{J=1}^{n_J^{(s,0)}} \mathrm{Re}\{v_J^{(s)}(\mathbf{x}_J^{(s,0)})\}\mathrm{Re}\{f_J^{(s,0)}\}. \tag{61}$$

The time-averaged power flow transmitted from $S^{(s)}$ to the Jth sky-hook controller is

$$P_J^{(s,0)} = \tfrac{1}{2}\mathrm{Re}\{f_J^{(s,0)} v_J^{*(s)}(\mathbf{x}_J^{(s,0)})\} \quad (J = 1, 2, \ldots, n_J^{(s,0)}). \tag{62}$$

The total time-averaged power flow transmitted from $S^{(s)}$ to all the $n_J^{(s,0)}$ sky-hook controllers is

$$P_a^{(s)} = \sum_{J=1}^{n_J^{(s,0)}} P_J^{(s,0)}. \tag{63}$$

3.4. Power flow absorption and dissipation

By using the power flow generation and transmission equations described previously, the instantaneous power flow absorbed and the time-averaged power flow dissipated in substructures $S^{(s)}$, the sky-hook controllers and the relative velocity feedback controllers can now be derived. Power flow absorption and dissipation quantities are used to investigate power flow control effectiveness. The aim of power flow control is to absorb vibratory energy or to minimize its transmission to vibration-sensitive regions of the structure through coupled active–passive control subsystems.

The instantaneous power flow $p_I^{(s,t)}$ and the time-averaged power flow $P_I^{(s,t)}$ absorbed by the Ith controller are given, respectively, by

$$p_I^{(s,t)} = \mathrm{Re}\{v_I^{(s)}(\mathbf{x}_I^{(s)}) - v_I^{(t)}(\mathbf{x}_I^{(t)})\}\mathrm{Re}\{f_I^{(s,t)}\}, \tag{64}$$

$$P_I^{(s,t)} = \tfrac{1}{2}\mathrm{Re}\{f_I^{(s,t)}[v_I^{*(s)}(\mathbf{x}_I^{(s)}) - v_I^{*(t)}(\mathbf{x}_I^{(t)})]\} \quad (I = 1, 2, \ldots, n_I^{(s,t)}). \tag{65}$$

The total instantaneous and the time-averaged power flows absorbed by all the $n_I^{(s,t)}$ active-passive controllers are expressed by the forms

$$p^{(s,t)} = \sum_{I=1}^{n_I^{(s,t)}} p_I^{(s,t)}, \quad P^{(s,t)} = \sum_{I=1}^{n_I^{(s,t)}} P_I^{(s,t)} \tag{66, 67}$$

The total instantaneous power flow $p_a^{(s)}$ and the time-averaged power flow $P_a^{(s)}$ absorbed by all the $n_J^{(s,0)}$ sky-hook controllers are given by Eqs. (62) and (63), respectively.

The total instantaneous power flow $p_{total}^{(s)}$ and the total time-averaged power flow $P_{total}^{(s)}$ entering substructure $S^{(s)}$ are given by

$$p_{total}^{(s)} = p_{L,in}^{(s)} + p_a^{(s)} + p^{(s)}, \quad P_{total}^{(s)} = P_{L,in}^{(s)} + P_a^{(s)} + P^{(s)}. \tag{68, 69}$$

Energy balances at each substructure imply that $P_{L,in}^{(s)}, P_a^{(s)}, P^{(s,t)}$ and $P_d^{(s)}$ satisfy

$$P_{L,in}^{(s)} + P_a^{(s)} + P^{(s)} + P_d^{(s)} = 0 \quad (s = 1, 2, \ldots, N), \tag{70}$$

where $P_d^{(s)}$ describing energy dissipation determined by Eq. (48c).

For the totally passive controlled system, the corresponding formulations are readily obtained by imposing $g_I^{(s,t)} = 0$ and $g_J^{(s,0)} = 0$ ($s = 1, 2, \ldots, N; I = 1, 2, \ldots, n_I^{(s,t)}; J = 1, 2, \ldots, n_J^{(s,0)}$) in these equations.

4. Dynamic transfer characteristics

4.1. Transmissibility

The conventional force transmissibility function is extended for the complex coupled structure–control system and defined by

$$T_{L_i I_j}^{(s,t)} = \left| F_{I_j}^{(t,s)} / F_{L_i}^{(s)} \right| \quad (i,j = 1, 2, 3; I = 1, 2, \ldots, N^{(t)}; L = 1, 2, \ldots, n^{(s)}, s = 1, 2, \ldots, N, t \in H^{(s)}). \tag{71}$$

Physically, the transmissibility function $T_{L_i I_j}^{(s,t)}$ represents the response force component in the direction $x_j^{(t)}$ at point $\mathbf{x}_I^{(t)}$ of substructure $S^{(t)}$ caused by a unit external excitation force component $F_{L_i}^{(s)}$ in the direction of $x_i^{(s)}$ at point $\mathbf{x}_L^{(s)}$ of substructure $S^{(s)}$.

4.2. Kinetic energy spectra

As it is widely used in vibration control engineering [7,12,19], the summation of the squared values of velocity amplitudes at suitable chosen positions in/on structures is often taken as a cost function. This is an approximation to the vibration energy of the structure as indicated in Ref. [7]. In this paper, the mounting positions $\mathbf{x}_I^{(t)}$ of the substructure $S^{(t)}$ are chosen to evaluate the control

performances and to estimate the kinetic energy of substructure $S^{(t)}$ produced by external excitation forces of frequency Ω. That is,

$$E_k^{(t)}(\Omega) = \sum_{I=1}^{n_I^{(s,t)}} \mathrm{Re}[v_i^{(t)}(\mathbf{x}_I^{(t)})]\mathrm{Re}[v_i^{(t)}(\mathbf{x}_I^{(t)})] \quad (t = 1, 2, \ldots, N). \tag{72}$$

4.3. Power flow transmission ratio

To study further the control efficiency of the different feedback control strategies, one also examines the control strategies from a power flow control viewpoint. The ratio of the total power flowing to the receiving substructure to the total input power by all the vibration sources from $S^{(s)}$ $(s = 1, 2, \ldots, N)$ can be used as evaluation functions.

The total time-averaged power flow input to the whole system by external excitation forces applied to all substructures $S^{(s)}$ is given by

$$P_{in} = \sum_{s=1}^{N} P_{in}^{(s)}, \tag{73}$$

The time-averaged power flow transmission ratio $R^{(s)}$ of substructure $S^{(s)}$ is defined by

$$R^{(s)} = \frac{P_d^{(s)}}{P_{in}}, \tag{74}$$

which represents the averaged power flows transmitted from the unit power flow input by vibration sources.

5. Numerical simulations

To demonstrate the applicability of the general mathematical model described in this paper, numerical simulations of a hybrid active/passive vibration isolation system were undertaken to investigate the dynamical characteristics, control mechanisms and efficiency of different structure–control systems. The chosen system is composed of three substructures in which two are rigid and one is elastic. Another motivation for selecting this example is to demonstrate how the formulations presented in this paper are readily extended for systems consisting of distributed and lumped substructures with multiple passive/active control subsystems.

Fig. 2 illustrates the details of this system. Two machines, treated as rigid bodies of mass densities $\rho^{(1)}$ and $\rho^{(2)}$, are mounted by four elastic cylindrical tubes to a simply supported flexible plate. The machines are subject to harmonic excitation forces $\mathbf{f}_1^{(1)} = f_{11}^{(1)} = 0 = f_{12}^{(1)} = \mathbf{f}_2^{(1)}, \mathbf{f}_2^{(1)} = f_{13}^{(1)} = F_{13}^{(1)} e^{j\Omega t}$ and $\mathbf{f}_1^{(2)} = f_{11}^{(2)} = 0 = f_{12}^{(2)} = \mathbf{f}_2^{(2)}, \mathbf{f}_2^{(2)} = f_{13}^{(2)} = F_{13}^{(2)} e^{j\Omega t}$. The supporting plate has dimensions $L_1^{(3)} = 1.8$ m, $L_2^{(3)} = 1.21$ m and $H^{(3)} = 0.005$ m with material properties $E^{(3)} = 2.16 \times 10^{11}\,\mathrm{N/m^2}$, $G^{(3)} = 8 \times 10^{10}\,\mathrm{N/m^2}$, $\mu^{(3)} = 0.3$, density $\rho^{(3)} = 7800\,\mathrm{kg/m^3}$ and structural damping factor $\eta^{(3)} = 0.005$. The elastic mounts or passive isolators, grouped in twos with each group supporting one machine, are idealized by identical cylindrical tubes of height $h = 0.206$ m inner and outer radii $r = 0.045$ m, $R = 0.051$ m with material characteristics $E_I = 2.254 \times 10^7\,\mathrm{N/m^2}$,

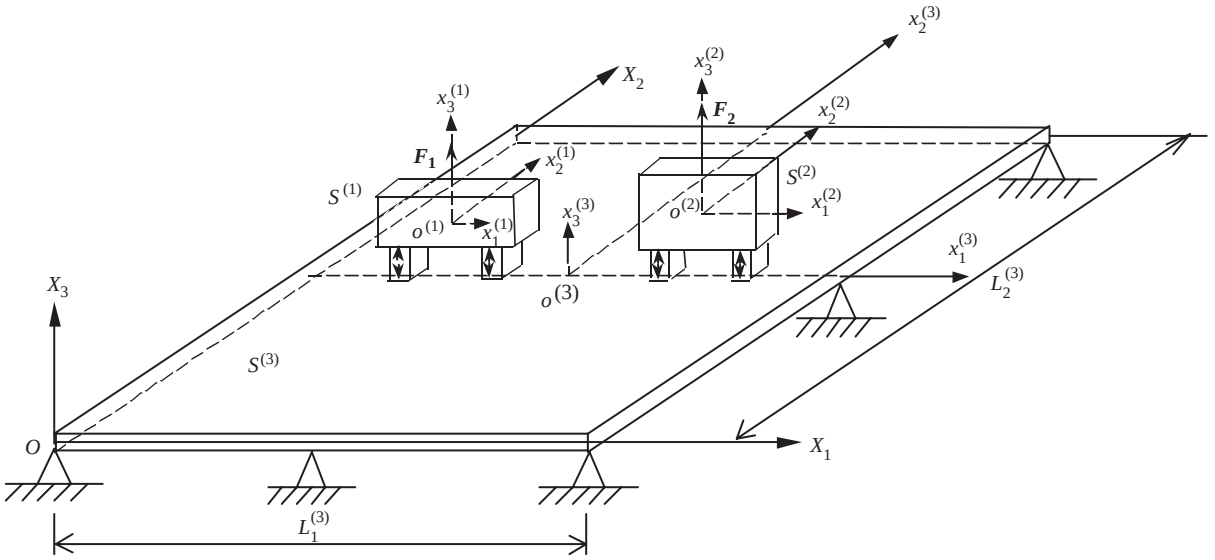

Fig. 2. An integrated structure-control system composed of three substructures and multiple active/passive/hybrid controllers.

$G_I = 7.83 \times 10^6\,\mathrm{N/m^2}$ and the Poisson ratio $\mu_I = 0.44$, respectively. Therefore the damping ratios of the isolators are $\eta_1^{(1,3)} = \eta_2^{(1,3)} = 0.47$ and $\eta_1^{(2,3)} = \eta_2^{(2,3)} = 0.47$.

Three active control strategies are considered including four-channel absolute, relative velocity feedback controls and their hybrid combination. The active control actuators, collocated with the passive isolators, are governed by a proportional feedback control law. To simplify calculations, the same feedback control gain g_r for the four relative velocity feedback controllers between the machines and the plate is used in each mount group, i.e., $g_r = g_I^{(1,3)} = g_I^{(2,3)}$ $(I = 1, 2)$. Similarly, the same feedback control gain g_a for the four sky-hook controllers at the mounting points of the plate is applied.

In the numerical simulations, transmissibility functions, time-averaged power flows and power flow transmission ratios for various cases are calculated and compared. Only low-frequency vibrations under 100 Hz were considered so that the machine structures could be modelled as rigid bodies and each mount as a massless isolator.

The local coordinate systems are denoted by $o^{(s)}$-$x_1^{(s)}x_2^{(s)}x_3^{(s)}$ $(s = 1, 2, 3)$ of which the origins $o^{(s)}$ are located at their centres of mass, respectively. The origin O of the global co-ordinate system O-$X_1X_2X_3$ is fixed at the left lower corner of the plate as shown in Fig. 2.

5.1. Input data

In the notation used in the theoretical formulations described in the paper, the data describing each substructure are listed as follows. This information covers the inputs required to commence the numerical calculation. The international system of units: mass (kg), length (m), time (s) and force (N) are used with no further explanation.

5.1.1. Substructure $S^{(1)}$

- Local co-ordinate system:
  global coordinates of the origin, $o^{(1)}(0.45, 0.605, 0.3585)$;
  transformation matrix, $\theta_{ij}^{(1)} = \delta_{ij}$.
- Number of external excitation force, $n^{(1)} = 1$:
  external excitation force vector, $\mathbf{f}_1^{(1)} = \mathbf{0} = \mathbf{f}_2^{(1)},\ \mathbf{f}_3^{(1)} = F_{13}^{(1)} e^{j\Omega t}$;
  local position of the force $f_{1i}^{(1)}$; $\mathbf{x}_1^{(1)} = [0, 0, 0.15]$.
- Mass density: $\rho^{(1)} = 545$.
- Dimensions of $S^{(1)}$: length $l^{(1)} = 0.5$, width $b^{(1)} = 0.4$, height $h^{(1)} = 0.3$;
- Natural frequencies and modes, $N^{(1)} = 2$;
  $\omega_1^{(1)} = 0,\ \varphi_{11}^{(1)} = \varphi_{21}^{(1)} = 0,\ \varphi_{31}^{(1)} = 1$;
  $\omega_2^{(1)} = 0,\ \varphi_{12}^{(1)} = x_3^{(1)},\ \varphi_{22}^{(1)} = 0,\ \varphi_{32}^{(1)} = -x_1^{(1)}$.
- Damping: $\eta^{(1)} = 0$.
- Local co-ordinates of mounting points at $S^{(1)}$:
  $\mathbf{x}_1^{(1,3)} = [-0.15, 0, -0.15], \quad \mathbf{x}_2^{(1,3)} = [0.35, 0, -0.15]$.

5.1.2. Substructure $S^{(2)}$

- Local co-ordinate system:
  global co-ordinates of the origin, $o^{(2)}(1.35, 0.605, 0.4085)$;
  transformation matrix, $\theta_{ij}^{(2)} = \delta_{ij}$.
- Number of external excitation force, $n^{(2)} = 1$:
  excitation force vector, $\mathbf{f}_1^{(2)} = \mathbf{0} = \mathbf{f}_2^{(2)},\ \mathbf{f}_3^{(2)} = F_{13}^{(2)} e^{j\Omega t}$;
  position vector of the force $f_{1i}^{(2)}, \mathbf{x}_1^{(2)} = [0,\ 0,\ 0.20]$.
- Mass density: $\rho^{(2)} = 545$.
- Dimensions of $S^{(2)}$: length $l^{(2)} = 0.5$, width $b^{(2)} = 0.4$, height $h^{(2)} = 0.4$.
- Natural frequencies and modes, $N^{(2)} = 2$;
  $\omega_1^{(2)} = 0,\ \varphi_{11}^{(2)} = \varphi_{21}^{(2)} = 0,\ \varphi_{31}^{(2)} = 1$;
  $\omega_2^{(2)} = 0,\ \varphi_{12}^{(2)} = x_3^{(2)}, \varphi_{22}^{(2)} = 0,\ \varphi_{32}^{(2)} = -x_1^{(2)}$.
- Damping: $\eta^{(2)} = 0$.
- Local co-ordinates of mounting points at $S^{(2)}$:
  $\mathbf{x}_1^{(2,3)} = [-0.20, 0, -0.20], \quad \mathbf{x}_2^{(2,3)} = [0.30, 0, -0.20]$.

5.1.3. Substructure $S^{(3)}$

- Local co-ordinate system:
  global co-ordinates of the origin, $o^{(3)}(0.9, 0.605, 0)$;
  transformation matrix, $\theta_{ij}^{(3)} = \delta_{ij}$.
- Number of external excitation force, $n^{(3)} = 0$.
- Mass density: $\rho^{(3)} = 7800$.
- Dimensions of $S^{(3)}$: length $L_1^{(3)} = 1.8$, width $L_2^{(3)} = 1.21$, thickness $H^{(3)} = 0.005$.
- Material properties: $E^{(3)} = 2.16 \times 10^{11}$, $G^{(3)} = 8 \times 10^{10}$, $\mu^{(3)} = 0.3$.
- Natural frequencies and modes, $N^{(3)} = 25$ (Table 1):

Table 1
Natural mode numbers of m and n

Modes	1	2	3	4	5	6	7	8	9	10	11	12	13	14	15	16	17	18	19	20	21	22	23	24	25
m	1	2	1	3	2	3	4	1	2	4	5	3	5	4	1	6	2	3	6	5	7	4	6	1	7
n	1	1	2	1	2	2	1	3	3	2	1	3	2	3	4	1	4	4	2	3	1	4	3	5	2

Natural frequencies:

$$f_{m,n}^{(3)} = \left[\left(\frac{m\pi^2}{L_1^{(3)}}\right) + \left(\frac{n\pi}{L_2^{(3)}}\right)^2\right]\sqrt{\frac{D}{p^{(3)}h^{(3)}}}, \quad \text{where } D = \frac{E^{(3)}(h^{(3)})^3}{12[1-(\mu^{(3)})^2]}.$$

Mode shapes:

$$\varphi_{3mn}^{(3)} = \sin\frac{m\pi\, x_1^{(3)}}{L_1^{(3)}}\sin\frac{n\pi\, x_2^{(3)}}{L_2^{(3)}}, \quad \varphi_{1mn}^{(3)} = 0 = \varphi_{2mn}^{(3)}.$$

- Structural damping factor: $\eta^{(3)} = 0.005$.
- Local co-ordinates of controllers' mounting points at $S^{(3)}$:
  no. 1 controller, $\mathbf{x}_1^{(3,1)} = [-0.15, 0, -0.356]$;
  no. 2 controller, $\mathbf{x}_2^{(3,1)} = [0.35, 0, -0.356]$;
  no. 3 controller, $\mathbf{x}_1^{(3,2)} = [-0.20, 0, -0.406]$;
  no. 4 controller, $\mathbf{x}_2^{(3,2)} = [0.30, 0, -0.406]$.

5.1.4. Active–passive controller system parameters:

- Number of controllers: $n_I^{(1,3)} = 2,\ n_I^{(2,3)} = 2$;
- Stiffness: $k_1^{(1,3)} = 1.36\times10^3\ \text{N/m} = k_2^{(2,3)},\ k_1^{(2,3)} = 1.56\times10^3\ \text{N/m} = k_2^{(2,3)}$;
- Damping: $\eta_1^{(1,3)} = 0.47 = \eta_2^{(1,3)},\ \eta_1^{(2,3)} = 0.47 = \eta_2^{(2,3)}$.
- Relative velocity feedback control gains: $g_1^{(1,3)} = g_2^{(1,3)} = 0,\ 10, g_1^{(2,3)} = g_2^{(2,3)} = 0,\ 10.$
- Absolute velocity feedback control gains: $g_1^{(3)} = g_2^{(3)} = 0,\ 100,\ 500, g_1^{(3)} = g_2^{(3)} = 0,\ 100,\ 500.$

5.2. Results and discussions

Figs. 3–8 show a selection of results derived from dynamic simulations of the described system. In these figures, the thick solid lines represent the case of pure passive control; the dash-dotted lines indicate the case of retrofitting relative velocity feedback controllers into the pure passive system; the dotted lines refer to the system in association with sky-hook controllers attached to the plate and introduced into the passive system; and the hybrid controls are represented by dashed lines.

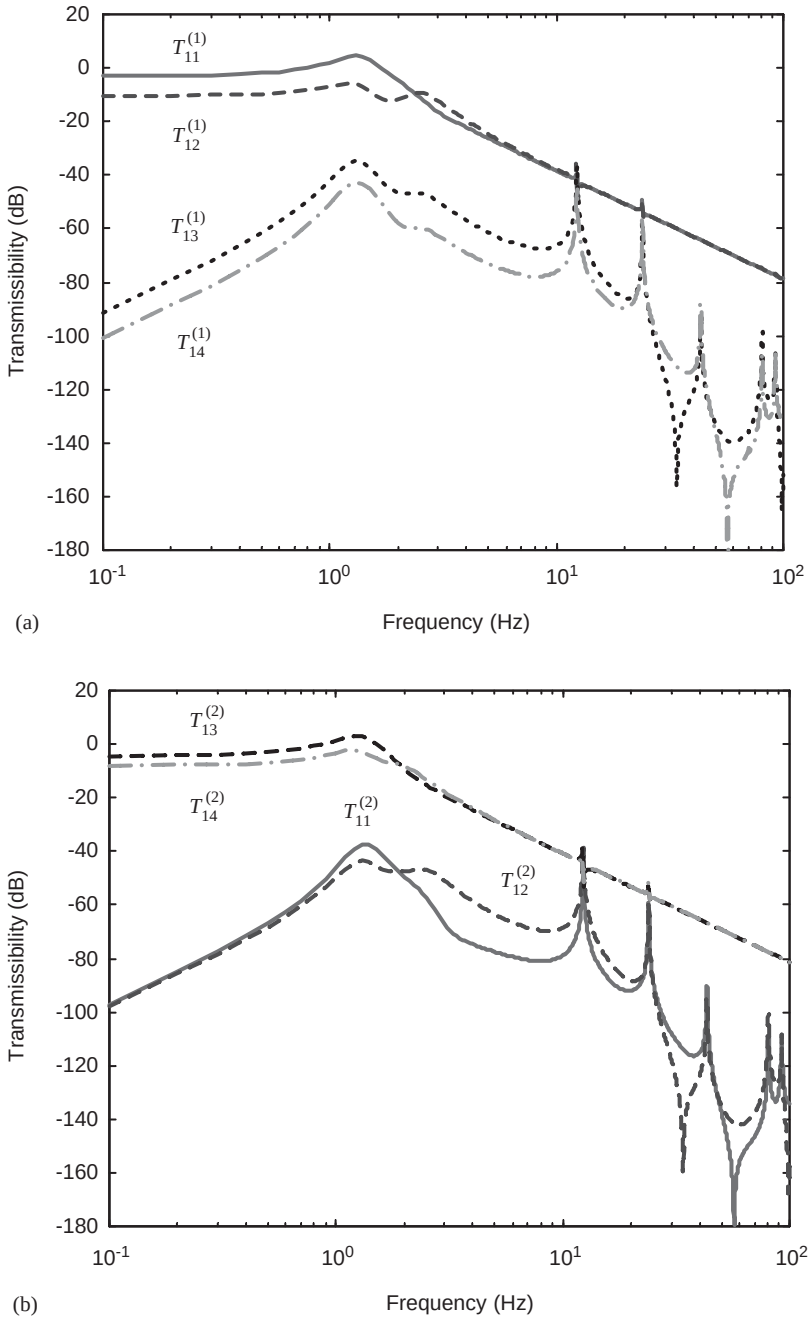

Fig. 3. The transmissibility functions for passive control system: (a) $F_{13}^{(1)}=1, F_{13}^{(2)}=0$; (b) $F_{13}^{(1)}=0$, $F_{13}^{(2)}=1$; $T_{1I}^{(s)}$ ($I=1,2,3,4$; $s=1,2$) represents the force transmitted to mounting points I on the plate due to a unit force $F_{13}^{(s)}=1$.

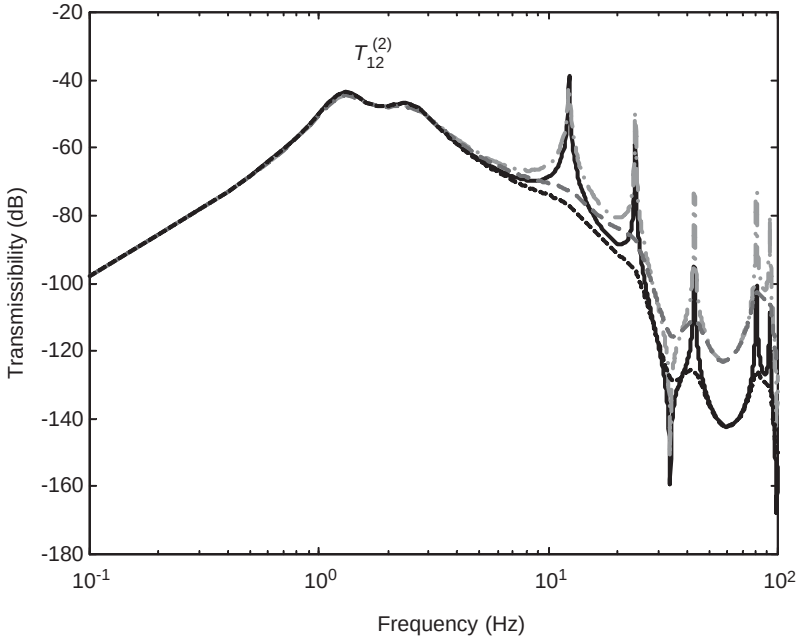

Fig. 4. Comparison of passive, active and hybrid control of transmissibility function $T_{12}^{(2)}$ ($F_{13}^{(1)} = 0, F_{13}^{(2)} = 1$): ———, passive; –·–·–·, $g_r = 10$; - - - - - -, $g_a = 500$; – – – –, $g_a = 500$, $g_r = 10$.

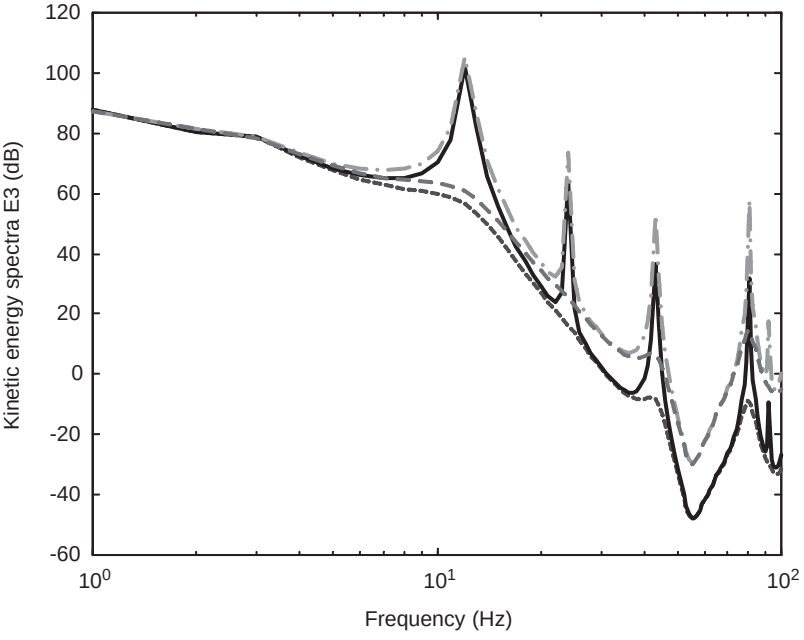

Fig. 5. Kinetic energy spectra $E_k^{(3)}$ for different control schemes ($F_{13}^{(1)} = 1, F_{13}^{(2)} = 1$): ———, passive; –·–·–·, $g_r = 10$; - - - - - -, $g_a = 500$; – – – –, $g_a = 500$, $g_r = 10$.

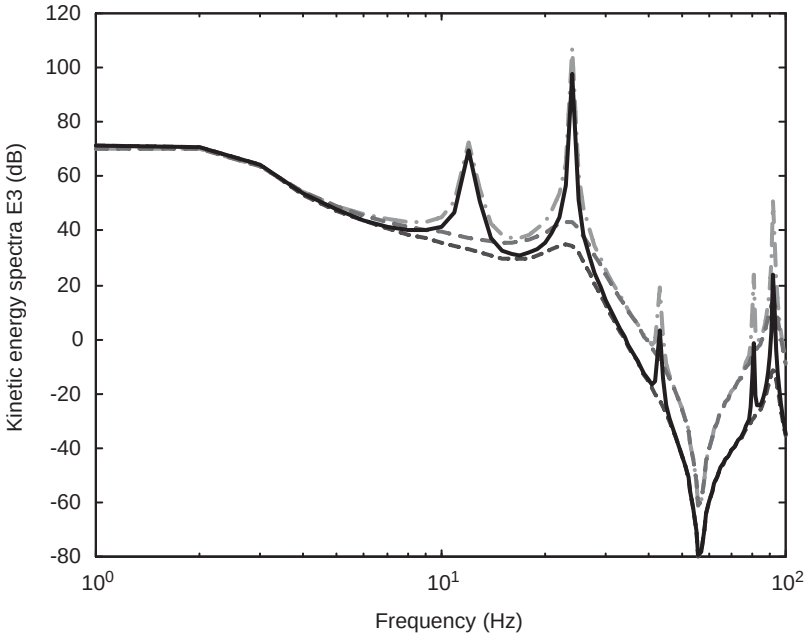

Fig. 6. Kinetic energy spectra $E_k^{(3)}$ for different control schemes ($F_{13}^{(1)} = 1, F_{13}^{(2)} = -1$): ———, passive; $-\cdot-\cdot-\cdot-$, $g_r = 10$; - - - - - - , $g_a = 500$; – – – – , $g_a = 500$, $g_r = 10$.

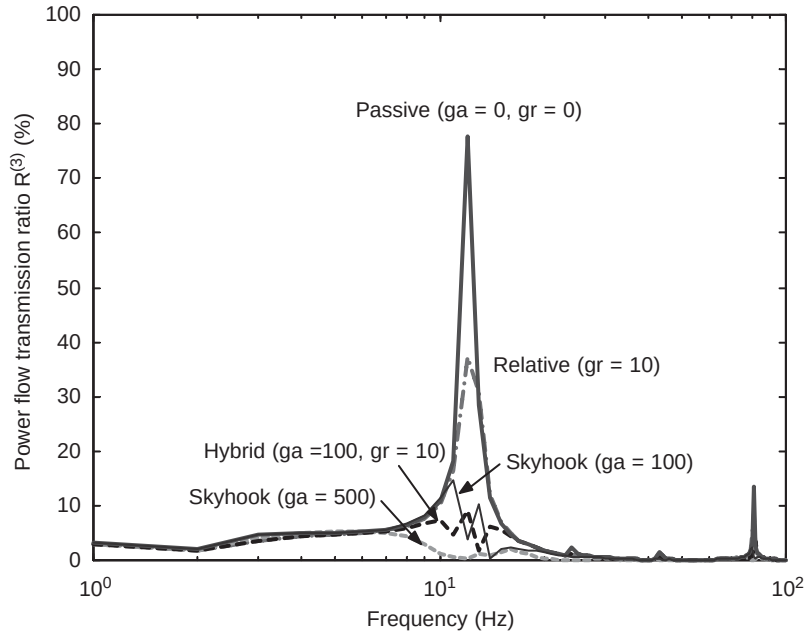

Fig. 7. Power flow transmission ratio $R^{(3)}\%$ ($F_{13}^{(1)} = 1, F_{13}^{(2)} = 1$).

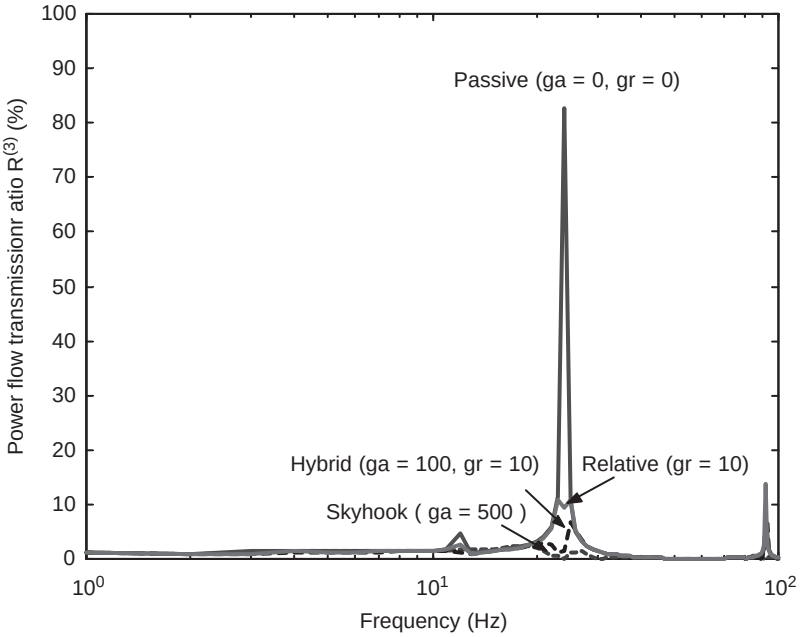

Fig. 8. Power flow transmission ratio $R^{(3)}\%$ ($F_{13}^{(1)}=1, F_{13}^{(2)}=-1$).

5.2.1. Transmissibility

The force transmissibility functions given in Eq. (71) now take the form $T_{1_3 I_3}^{(s,3)} = \left|F_{I_3}^{(s,3)}/F_{1_3}^{(s)}\right|$ ($s=1,2; I=1,2,3,4$) for the model represented in Fig. 2. For convenience of presentation in Figs. 3 and 4, the notations $T_{1I}^{(s)} = T_{1_3 I_3}^{(s,3)}$ ($s=1,2; I=1,2,3,4$) are used. These four interesting points representing by subscript ($I=1,2,3,4$) are the mounting positions on the plate as shown in Fig. 2.

Figs. 3(a) and (b) show the transmissibility functions (in decibels, i.e., $20\log(T_{1I}^{(s)})$) corresponding to the unit driving forces $F_{13}^{(1)}=1, F_{13}^{(2)}=0$ and $F_{13}^{(1)}=0, F_{13}^{(2)}=1$, respectively, for the passive control system. It is seen from these figures that the passive isolation control suppresses the dynamic forces transmitted to the receiver, especially in the range of high frequencies as confirmed by classical theory [2,3,5]. It is very interesting to observe that the transmissibility curves $T_{1I}^{(1)}$ ($I=1,2$) in Fig. 3(a) and $T_{1I}^{(2)}$ ($I=3,4$) in Fig. 3(b) are less affected by the dynamic characteristics of the plate structure, whereas the curves $T_{1I}^{(1)}$ ($I=3,4$) in Fig. 3(a) and $T_{1I}^{(2)}$ ($I=1,2$) in Fig. 3(b) exhibit many resonance peaks corresponding to the resonance of the flexible plate. This is because the force transmission paths in the latter cases include the elastic plate and therefore the effect of the dynamic characteristics of the plate is more obvious.

As an example, Fig. 4 shows the effect of the three different active control strategies to the transmissibility function $T_{12}^{(2)}$ to compare active control and passive efficiencies.

It is shown in this figure that the most significant attenuation of the force transmissibility, affected by the resonant peaks of the flexible base, is achieved by using sky-hook controllers ($g_a=500$). However, the transmissibility is amplified in the range of higher frequencies under the

relative velocity feedback control, even using a small control gain $g_r = 10$. This is because the relative velocity feedback controllers generate active damping in the mountings hence increasing the transmitted force to the plate.

5.2.2. Kinetic energy

Figs. 5 and 6 show the kinetic energy spectra of the plate (substructure $S^{(3)}$) produced by the two sets of external excitation forces $F_{13}^{(1)} = 1 = F_{13}^{(2)}$ and $F_{13}^{(1)} = 1 = -F_{13}^{(2)}$ applied to substructures $S^{(1)}$ and $S^{(2)}$, respectively. The control efficiency of the passive, active and hybrid control schemes are compared in these figures. As observed in Fig. 4, the sky-hook controllers ($g_a = 500$) on the plate are the most effective way to suppress the kinetic energy of the receiving plate. Whereas the relative active feedback control deteriorates control efficiency in comparison to that for the passive case as shown by the dash-dotted line in the figures ($g_r = 10$). Further detailed calculations demonstrate that the larger the control gain g_r, the poorer the control efficiency.

5.2.3. Power flow transmission ratio

The control strategies are now examined from a power flow control viewpoint, through the ratio $R^{(3)}$. This denotes the total time-averaged power flowing to the receiving substructure $S^{(3)}$ to the total input power generated by the two vibration sources from $S^{(1)}$ and $S^{(2)}$. Figs. 7 and 8 present comparisons of the power transmission ratio $R^{(3)}$ for various active velocity feedback controllers retrofitted to the pure passive control system subject to the respective excitation forces $F_{13}^{(1)} = 1 = F_{13}^{(2)}$ and $F_{13}^{(1)} = 1 = -F_{13}^{(2)}$. The influences of feedback gain values in the different controllers are shown in the figures.

It is demonstrated that all the three active feedback control schemes are effective in reducing the power transmission from vibration sources to the receiving structure. The sky-hook controllers again show the best results. It can be seen that passive isolators only dissipate 20% power from the vibration sources whereas 95% power is dissipated by retrofitting active sky-hook controllers with a gain $g_a = 500$ into the pure passive system.

Although relative velocity feedback controllers induce an amplification of the force amplitude transmitted to the receiver as shown in Figs. 3 and 4 and produce a larger kinetic energy in the base structure as presented in Figs. 5 and 6, the time-averaged power flow transmission ratio is also decreased in comparison with the passive one as shown in Figs. 7 and 8. This is because the relative velocity feedback controllers produce additional active damping to dissipate the vibration power input of the vibration sources. This demonstrates, in general, that retrofitting active control systems into passive ones provides further substantial reductions of the power flow transmission.

6. Conclusions

A generalized unifying mathematical model of a multiple channel passive/active/hybrid integrated structure–control system consisting of any number of flexible/rigid substructures $S^{(s)}$ ($s = 1, 2, \ldots, N$) and any number of controllers of various types is developed to describe the dynamic characteristics, vibration control efficiency and multiple channel power flow

transmissions in complex dynamical coupling systems. The theoretical model encompasses the following cases:

(1) The substructures are flexible with arbitrary configuration and generalized boundary conditions. If deformation of a substructure is neglected, it reduces to a rigid body. Furthermore, it degenerates into a mass point if its size is not considered.

(2) The loads applied to any point $\mathbf{x}_L^{(s)}$ of substructure $S^{(s)}$ are generalized multiple dimensional in form. These loads can be applied to any points on the surfaces of substructures or in the substructures.

(3) All $n_J^{(s,0)}$ ($J = 1, 2, \ldots, n_J^{(s,0)}$) sky-hook feedback controllers, fixed between any point in or on substructures $S^{(s)}$ ($s = 1, 2, \ldots, N$) and any point on the earth, provide active control damping proportional to the absolute velocity of substructures $S^{(s)}$. All $n_I^{(s,t)}$ relative velocity feedback controllers, producing active control damping proportional to the relative velocities between the two substructures $S^{(s)}$ and $S^{(t)}$, can be arbitrarily arranged between them. The spatial orientations of all the active/passive controllers are arbitrary and determined by their directional cosine vectors. This provides flexibility in the control design to adjust the positions and directions of the passive and active controllers to obtain optimal control effectiveness.

In consideration of the representative substructures described in this paper, the formulations developed herein can be readily applied to model a large complex system consisting of many substructures.

The generality of the theory is demonstrated through an example of hybrid control systems consisting of flexible and rigid substructures. This provides a basis to develop a general computer program that allows the user to build arbitrarily complex linear control models using simple commands and inputs. This generalized model covers a wide a range of dynamic systems and control models studied in the literature. It permits description of complicated substructures encountered in practical industrial applications. It allows the study of different control strategies: i.e., passive, active and hybrid, from the perspectives of both conventional dynamic response/force minimization and energy flow control. It provides a means to understand control mechanisms and to assess control efficiency when controllers are integrated into complex coupled dynamical systems constructed of distributed substructures. The formulations of mobility, receptance, transmissibility, power flow transmission functions for general three-dimensional elastic structures in association with multi-dimensional active–passive control subsystems are presented to characterize the dynamical behaviour of complex integrated structure–control systems and their dynamic interactions. All the power flow components associated with all the excitation force components from each passive/active/hybrid mounting or controller can be evaluated.

Numerical applications of the approach are presented to illustrate the method, to validate it against other numerical experiments and to demonstrate control mechanisms and their efficiencies associated with complex coupled dynamical systems. Numerical simulations demonstrate that the three control strategies efficiently suppress the resonance modes of the integrated structure–control system reducing the maximum displacement response and corresponding power flow in the low-frequency band and hence significantly improve the performance of the original passive control system. It is further demonstrated by numerical results the importance of incorporating the dynamic characteristics of the flexible structure in evaluating active control efficiency and effectiveness and the study provides theoretical and practical guidelines for vibration control design.

Appendix A. The orthogonality of natural modes and orthogonalization of modes of the same frequency

A traditional tensor analysis notation [30] is used to develop the mathematical model described in this paper. For example, stress tensor σ_{ij}, displacement vector u_i, elastic tensor E_{ijkl}, etc. This approach is continued to describe the dynamic characteristics of a general elastic structure/body. Fig. 9 illustrates the structure occupying a domain V subject to fixed boundary S_u and free boundary S_T with its unit normal vector v_i pointing outwards. The governing equations describing the natural vibrations of the elastic body are the following:

$$\textit{dynamic equation}: \quad \sigma_{ij,j} = \rho u_{i,tt}, \quad \mathbf{x} \in V, \tag{A.1}$$

$$\textit{constitutive equation}: \quad \sigma_{ij} = E_{ijkl}\varepsilon_{kl}, \quad \mathbf{x} \in V, \tag{A.2}$$

$$\textit{geometric relation}: \quad \varepsilon_{kl} = \tfrac{1}{2}(u_{k,l} + u_{l,k}), \quad \mathbf{x} \in V, \tag{A.3}$$

$$\textit{boundary conditions}: \quad \sigma_{ij}v_j = 0, \quad \mathbf{x} \in S_T; \quad u_i = 0, \quad \mathbf{x} \in S_u. \tag{A.4}$$

The substitution of Eqs. (A.2) and (A.3) into Eqs. (A.1) and (A.4) gives

$$E_{ijkl}u_{k,lj} = \rho u_{i,tt}, \quad \mathbf{x} \in V, \qquad E_{ijkl}u_{k,l}v_j = 0, \quad \mathbf{x} \in S_T, \qquad u_i = 0, \quad \mathbf{x} \in S_u. \tag{A.5}$$

The natural vibration of the elastic structure is given by $u_i = U_i e^{j\omega t}$ from which it follows that

$$E_{ijkl}U_{k,lj} = -\omega^2 U_i \rho, \quad E_{ijkl}U_{k,l}v_j = 0, \quad U_i = 0. \tag{A.6}$$

Eq. (A.6) defines a typical eigenvalue problem [31]. The solution of this equation determines the natural frequencies and the corresponding natural modes. The othogonality of the natural modes are discussed now.

Case I: $\omega^{<p>} \neq \omega^{<q>}$. It is assumed that $U_i^{<p>}$ and $U_i^{<q>}$ are two arbitrary natural vibration modes with their corresponding natural frequencies $\omega^{<p>}$ and $\omega^{<q>}$ ($\omega^{<p>} \neq \omega^{<q>}$), respectively, satisfying Eq. (A.6), i.e.,

$$E_{ijkl}U_{k,lj}^{<p>} = -(\omega^{<p>})^2 \rho U_i^{<p>}, \quad E_{ijkl}U_{k,l}^{<p>}v_j = 0, \quad U_i^{<p>} = 0, \tag{A.7}$$

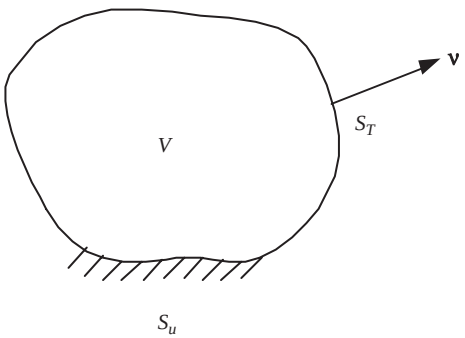

Fig. 9. A general elastic body occupying domain V with displacement boundary S_u, traction boundary S_T and unit normal vector $\mathbf{v}$.

and

$$E_{ijkl}U_{k,lj}^{<q>} = -[\omega^{<q>}]^2\rho U_i^{<q>}, \quad E_{ijkl}U_{k,l}^{<q>}v_j = 0, \quad U_i^{<q>} = 0. \tag{A.8}$$

Multiplying the first equation in Eq. (A.7) by $U_i^{<q>}$, integrating over the domain V, using the Green theorem and the boundary conditions in the second and third equations of (A.7), one obtains

$$\int_V U_{i,j}^{<q>}E_{ijkl}U_{k,l}^{<p>}\,\mathrm{d}V = (\omega^{<p>})^2\int_V \rho U_i^{<q>}U_i^{<p>}\,\mathrm{d}V. \tag{A.9}$$

Similarly, from Eq. (A.8), it follows that

$$\int_V U_{i,j}^{<p>}E_{ijkl}U_{k,l}^{<q>}\,\mathrm{d}V = (\omega^{<q>})^2\int_V \rho U_i^{<p>}U_i^{<q>}\,\mathrm{d}V. \tag{A.10}$$

Application of the relation $E_{ijkl} = E_{klij}$ and the summation convention for tensors gives

$$\int_V U_{i,j}^{<q>}E_{ijkl}U_{k,l}^{<p>}\,\mathrm{d}V = \int_V U_{k,l}^{<q>}E_{ijkl}U_{i,j}^{<p>}\,\mathrm{d}V. \tag{A.11}$$

Subtracting Eq. (A.10) from Eq. (A.9) one finds

$$\{(\omega^{<p>})^2 - (\omega^{<q>})^2\}\int_V \rho U_i^{<p>}U_i^{<q>}\,\mathrm{d}V = 0. \tag{A.12}$$

Because $\omega^{<p>} \neq \omega^{<q>}$, it thus follows that

$$\int_V \rho U_i^{<p>}U_i^{<q>}\,\mathrm{d}V = 0, \quad \int_V U_{i,j}^{<p>}E_{ijkl}U_{k,l}^{<q>}\,\mathrm{d}V = 0, \tag{A.13, A.14}$$

from Eq. (A.9) or (A.10).

Finally, the orthogonality of the natural modes of the three-dimensional elastic structure can be represented as

$$\int_V \rho U_i^{<p>}U_i^{<q>}\,\mathrm{d}V = \delta_{pq}M^{<p>}, \quad \int_V U_{i,j}^{<p>}E_{ijkl}U_{k,l}^{<q>}\,\mathrm{d}V = \delta_{pq}K^{<p>}, \tag{A.15, A.16}$$

where δ_{pq} is the Kronecker delta and $M^{<p>}$ is the generalized mass of the mode. The generalized stiffness $K^{<p>}$ takes the forms

$$K^{<p>} = \int_V U_{i,j}^{<p>}E_{ijkl}U_{k,l}^{<p>}\,\mathrm{d}V = (\omega^{<q>})^2M^{<p>}. \tag{A.17}$$

Case II: $\omega^{<p>} = \omega^{<q>}$. In this case, Eq. (A.13) may not be valid, i.e.,

$$M^{<pq>} = \int_V \rho U_i^{<p>}U_i^{<q>}\,\mathrm{d}V \neq 0. \tag{A.18}$$

An orthogonal mode function $\bar{U}_i^{<q>}$ can be constructed by using the Gram–Schmidt orthogonalization procedure [32]. By assuming that

$$\bar{U}_i^{<q>} = U_i^{<p>} + \alpha U_i^{<q>}, \tag{A.19}$$

where α is a constant to be determined by the orthogonal condition,

$$\int_V \rho U_i^{<p>}\bar{U}_i^{<q>}\,\mathrm{d}V = \int_V \rho U_i^{<p>}(U_i^{<p>} + \alpha U_i^{<q>})\,\mathrm{d}V = 0. \tag{A.20}$$

Therefore, one obtains that

$$\alpha = -\frac{M^{<p>}}{M^{<pq>}}, \tag{A.21}$$

and the orthogonal mode function in Eq. (A.19) for which the generalized mass is

$$\bar{M}^{<q>} = \int_V \rho \bar{U}_i^{<q>} \bar{U}_i^{<q>} \, \mathrm{d}V = -M^{<p>} + \alpha^2 M^{<q>}. \tag{A.22}$$

Case III: $\omega^{<p>} = \omega^{<q>} = \omega^{<r>}$. For this case, there are three modes with the same frequency. The orthogonal mode function given in Eq. (A.19) is still valid. The third orthogonal mode can be constructed in the form

$$\bar{U}_i^{<r>} = \bar{U}_i^{<q>} + \beta U_i^{<p>} + \gamma U_i^{<r>}, \tag{A.23}$$

which satisfies the orthogonality relations

$$\begin{aligned} \int_V \rho \bar{U}_i^{<q>\mathrm{T}} \bar{U}_i^{<r>} \, \mathrm{d}V &= \int_V \rho \{ \bar{U}_i^{<q>\mathrm{T}} \bar{U}_i^{<q>} + \beta \bar{U}_i^{<q>\mathrm{T}} U_i^{<p>} + \gamma \bar{U}_i^{<q>\mathrm{T}} U_i^{<r>} \} \, \mathrm{d}V \\ &= \bar{M}^{<q>} + \gamma \bar{M}^{<qr>} = 0, \end{aligned} \tag{A.24a}$$

$$\begin{aligned} \int_V \rho U_i^{<p>\mathrm{T}} \bar{U}_i^{<r>} \, \mathrm{d}V &= \int_V \rho \{ U_i^{<p>\mathrm{T}} \bar{U}_i^{<q>} + \beta U_i^{<p>\mathrm{T}} U_i^{<p>} + \gamma U_i^{<p>\mathrm{T}} U_i^{<r>} \} \, \mathrm{d}V \\ &= \beta M^{<p>} + \gamma M^{<pr>} = 0, \end{aligned} \tag{A.24b}$$

from which one obtains

$$\beta = -\frac{\bar{M}^{<q>}}{\bar{M}^{<qr>}}, \quad \gamma = -\frac{\beta M^{<p>}}{M^{<pr>}}, \tag{A.25}$$

where

$$\bar{M}^{<qr>} = \int_V \rho \bar{U}_i^{<q>\mathrm{T}} U_i^{<r>} \, \mathrm{d}V. \tag{A.26}$$

The corresponding generalized mass for the third mode function is

$$\begin{aligned} \bar{M}^{<r>} &= \int_V \rho \bar{U}_i^{<r>} \bar{U}_i^{<r>} \, \mathrm{d}V \\ &= \bar{M}^{<q>} + \beta^2 M^{<p>} + \gamma^2 M^{<r>} + 2\gamma \bar{M}^{<qr>} + 2\beta\gamma M^{<pr>}. \end{aligned} \tag{A.27}$$

If there are more modes with the same frequency, all orthogonal modes can be constructed by this method.

Case IV: rigid modes. If there is no displacement boundary condition on S_u described in Eq. (A.4), there exists six rigid modes of motion of the structure. These rigid modes have the same frequency $\omega^{<0>} = 0$. The orthogonal rigid modes can be constructed in the same way as in cases II and III. Let one assume that the origin of the reference co-ordinate system is located at the centre of mass of the structure. The displacement u_i produced by a small rigid motion can be calculated by a summation of the translation of the mass centre and the rotation about this centre [33], i.e.,

$$u_i = u_i^c + e_{ijk}\theta_j x_k, \tag{A.28}$$

where u_i^c represents the displacement vector of the centre of mass of the body and θ_j denotes the small rotation vector of the body about the centre of mass. The kinetic energy of the body is given by

$$T = \tfrac{1}{2}\int_V \rho \dot{u}_i \dot{u}_i \, \mathrm{d}V = \tfrac{1}{2}\int_V \rho \dot{u}_i^c \dot{u}_i^c \, \mathrm{d}V + \int_V \rho \dot{u}_i^c e_{ijk} \dot{\theta}_j x_k \, \mathrm{d}V + \tfrac{1}{2}\int_V \rho e_{ijk} e_{ilm} \dot{\theta}_j \dot{\theta}_l x_k x_m \, \mathrm{d}V. \tag{A.29}$$

Since the origin of the coordinate system is located at the centre of mass of the structure, the middle integration on the right side vanishes. Using the $e-\delta$ relation $e_{ijk}e_{ilm} = \delta_{jl}\delta_{km} - \delta_{jm}\delta_{kl}$ [5], one finds that

$$T = \tfrac{1}{2}\dot{u}_i^c M \dot{u}_i^c + \tfrac{1}{2}\dot{\theta}_i I_{ij} \dot{\theta}_j, \tag{A.30}$$

where M and I_{ij} represent the total mass and the moment matrix of inertia of the structure, respectively, which are given by

$$M = \int_V \rho \mathrm{d}V, \quad I_{ij} = \int_V \rho(\delta_{ij} x_k x_k - x_i x_j) \, \mathrm{d}V. \tag{A.31a, b}$$

By assuming the three displacement u_i^c of the centre of mass and the small rotation θ_j to be the generalized coordinates, one derives the six rigid modes:

$$\varphi^{<1>\mathrm{T}}(\mathbf{x}) = [1,0,0], \quad \varphi^{<2>\mathrm{T}}(\mathbf{x}) = [0,1,0], \quad \varphi^{<3>\mathrm{T}}(\mathbf{x}) = [0,0,1], \tag{A.32a}$$

$$\varphi^{<4>\mathrm{T}}(\mathbf{x}) = [0,-x_3,x_2], \quad \varphi^{<5>\mathrm{T}}(\mathbf{x}) = [x_3,0,-x_1], \quad \varphi^{<6>\mathrm{T}}(\mathbf{x}) = [-x_2,x_1,0]. \tag{A.32b}$$

If the co-ordinate system is the principal axis system of inertia of the structure, $I_{ij} = 0$ $(i \neq j)$, these six rigid modes are orthogonal. In general cases, the three translation modes in Eq. (A.32a) are orthogonal to each other and also orthogonal to the three rotational modes in Eq. (A.32b). However, the three rotational modes do not satisfy the orthogonality relations. The orthogonal modes can be constructed using the method describing in cases II and III. These are

$$\bar{\varphi}^{<5>}(\mathbf{x}) = \varphi^{<4>}(\mathbf{x}) + \alpha\varphi^{<5>}(\mathbf{x}), \tag{A.33a}$$

$$\bar{\varphi}^{<6>}(\mathbf{x}) = \bar{\varphi}^{<5>}(\mathbf{x}) + \beta\varphi^{<4>}(\mathbf{x}) + \gamma\varphi^{<6>}(\mathbf{x}), \tag{A.33b}$$

$$\alpha = -I_{11}/I_{12}, \quad \beta = -\gamma I_{13}/I_{11}, \quad \gamma = -\bar{I}_{22}/\bar{I}_{23}, \tag{A.33c}$$

$$\bar{I}_{22} = \int_V \rho \bar{\varphi}^{<5>\mathrm{T}} \bar{\varphi}^{<5>} \, \mathrm{d}V = -I_{11} + \alpha^2 I_{22}, \quad \bar{I}_{23} = \int_V \rho \bar{\varphi}^{<5>\mathrm{T}} \varphi^{<6>} \, \mathrm{d}V = I_{13} + \alpha I_{23}, \tag{A.33d}$$

$$\bar{I}_{33} = \int_V \rho \bar{\varphi}^{<6>\mathrm{T}} \bar{\varphi}^{<6>} \, \mathrm{d}V = \bar{I}_{22} + \beta^2 I_{11} + \gamma^2 I_{33} + 2\gamma\bar{I}_{23} + 2\beta\gamma I_{13}. \tag{A.33e}$$

The six orthogonal rigid modes described in Eqs. (A.32a), (A.32b.1) and (A.33a, b) are now derived for which the inertia matrix is a diagonal matrix

$$\bar{M} = \mathrm{diag}(M, M, M, I_{11}, \bar{I}_{22}, \bar{I}_{33}). \tag{A.34}$$

Appendix B. Nomenclature

$\mathbf{A}^{(s,s)}, \mathbf{A}^{(s,t)}$	help matrices
$\mathbf{B}_i^{(s)}$	transformation matrix between the physical excitation forces and the generalized forces
$c_I^{(s,t)} = c_I^{(t,s)}$	damping coefficient in the Ith control subsystem between substructures $S^{(s)}$ and $S^{(t)}$
$c_J^{(s,0)}$	viscous damping coefficient of sky-hook controller on substructure $S^{(s)}$
D	plate flexural rigidity
$E_{ijkl}^{(s)}$	tensor of elastic moduli of $S^{(s)}$
$E_{ijkl}^{*(s)}$	tensor of complex elastic moduli of $S^{(s)}$ $(= E_{ijkl}^{(s)}(1 + \mathrm{j}\eta^{(s)}))$
$E_k^{(t)}$	kinetic energy of $S^{(t)}$
$G^{(s)}$	shear moduli of $S^{(s)}$
$\mathbf{f}_i^{(s)}$	column vector of external exciting force applied to $S^{(s)}$ $(= f_{1i}^{(s)}, \ldots, f_{Li}^{(s)}, \ldots, f_{n^{(s)}i}^{(s)\,\mathrm{T}})$
$f_{Li}^{(s)}$	Lth exciting force of $S^{(s)}$
$f_{pI}^{(s,t)}$	Ith passive coupling force between the two substructures $S^{(s)}$ and $S^{(t)}$
$f_{aI}^{(s,t)}$	active control force associated with the Ith relative velocity feedback controller
$f_{m,n}^{(3)}$	natural frequency of plate substructure $S^{(3)}$
$\mathbf{F}_i^{(s)}$	column vector of excitation force amplitude of $S^{(s)}$ $(\mathbf{f}_i^{(s)} = \mathbf{F}_i^{(s)} \mathrm{e}^{\mathrm{j}\Omega t})$
$F_{Li}^{(s)}$	amplitude of the Lth exciting force of $S^{(s)}$ $(f_{Li}^{(s)} = F_{Li}^{(s)} \mathrm{e}^{\mathrm{j}\Omega t})$
$F_{L_i}^{(s)}$	external excitation force component in the direction of $\mathbf{x}_i^{(s)}$ at point $\mathbf{x}_L^{(s)}$ of $S^{(s)}$
$g_I^{(s,t)}$	relative velocity feedback control gain, $g_I^{(s,t)} = g_I^{(t,s)}$
$g_J^{(s,0)}$	absolute velocity feedback control gain
$H^{(s)}$	a set of numbers identifying the substructures connected to substructure $S^{(s)}$
$\mathbf{I}$	unit matrix
j	$= \sqrt{-1}$
$k_I^{(s,t)} = k_I^{(t,s)}$	stiffness of the spring in the Ith control subsystem between substructures $S^{(s)}$ and $S^{(t)}$
$\mathbf{K}^{(s)}$	stiffness matrix of $S^{(s)}$
$\mathbf{M}^{(s)}$	mass matrix of $S^{(s)}$
$n^{(s)}$	number of excitation forces applied to $S^{(s)}$
$n_I^{(s,t)}$	number of passive/active/hybrid control subsystem between $S^{(s)}$ and $S^{(t)}$
$n_J^{(s,0)}$	number of sky-hook control subsystem on $S^{(s)}$
N	number of substructures
$N^{(s)}$	number of the retained natural mode of $S^{(s)}$
p	instantaneous power
p_i	energy flow density vector
$p_i^{(s)}$	energy flow density vector at any point on/in $S^{(s)}$
$p_I^{(s,t)}$	instantaneous power flow transmission through the Ith control subsystem between $S^{(s)}$ and $S^{(t)}$
$p^{(s)}$	total instantaneous power transmitting from $S^{(s)}$ through all the $n_I^{(s,t)}$ controllers

$p_{L,in}^{(s)}$ Lth instantaneous input power flow by external excitation force $f_{Li}^{(s)}$ at the input point $\mathbf{x}_L^{(s)}$ on the boundary $S_T^{(s)}$ of $S^{(s)}$

$p_{in}^{(s)}$ total instantaneous input power by external excitation force into $S^{(s)}$

$p_{total}^{(s)}$ total instantaneous power flow entering into $S^{(s)}$

$p_I^{(s,t)}$ instantaneous power absorbed by the Ith control subsystem between $S^{(s)}$ and $S^{(t)}$

$p^{(s,t)}$ total instantaneous power absorbed by all the $n_I^{(s,t)}$ control subsystems between $S^{(s)}$ and $S^{(t)}$

$p_J^{(s,0)}$ instantaneous power transmitting from $S^{(s)}$ to the Jth sky-hook controller

$p_a^{(s)}$ total instantaneous power transmitting from $S^{(s)}$ to all the $n_J^{(s,0)}$ sky-hook controllers

P time-averaged power flow

$P_{L,in}^{(s)}$ time-averaged input power flow by external excitation force $f_{Li}^{(s)}$

$P_{in}^{(s)}$ total time-averaged input power flow into $S^{(s)}$

$P_I^{(s,t)}$ time-averaged power flow transmission through the Ith control subsystem between $S^{(s)}$ and $S^{(t)}$

$P^{(s)}$ total time-averaged power transmitting from $S^{(s)}$ through all the $n_I^{(s,t)}$ controllers

$P_d^{(s)}$ energy dissipation of $S^{(s)}$

$P_{total}^{(s)}$ total time-averaged power flow entering into $S^{(s)}$

$P^{(s,t)}$ total time-averaged power absorbed by all the $n_I^{(s,t)}$ control subsystems between $S^{(s)}$ and $S^{(t)}$

$P_J^{(s,0)}$ time-averaged power transmitting from $S^{(s)}$ to the Jth sky-hook controller

$P_a^{(s)}$ total time-averaged power transmitting from $S^{(s)}$ to all the $n_J^{(s,0)}$ sky-hook controllers

$q_{N^{(s)}}$ generalized co-ordinate of $S^{(s)}$

$\mathbf{q}^{(s)}(t)$ generalized co-ordinate column vector $(= [q_1, q_2, \ldots, q_{N^{(s)}}]^{(s)\mathrm{T}})$

$\mathbf{Q}^{(s)}$ amplitude of the generalized coordinate column vector $\mathbf{q}^{(s)}(t)$

$R^{(s)}$ time-averaged power flow transmission ratio of $S^{(s)}$

$S^{(s)}$ sth substructure $(s = 1, 2, \ldots, N)$

$S_u^{(s)}$ displacement boundary of $S^{(s)}$

$S_T^{(s)}$ traction boundary of $S^{(s)}$

t time variable

$T_{L_iI_j}^{(s,t)}$ force transmissibility functions

$u_i^{(s)}$ displacement vector of $S^{(s)}$

$v_i^{(s)}$ velocity vector of $S^{(s)}$

$V^{(s)}$ solid domain of $S^{(s)}$

$x_i^{(s)}$ local co-ordinates of $S^{(s)}$

$\mathbf{x}_L^{(s)}$ acting point of the Lth exciting force $f_{Li}^{(s)} = F_{Li}^{(s)} \mathrm{e}^{\mathrm{j}\Omega t}$, $(L = 1, 2, \ldots, n^{(s)})$

$\mathbf{x}_I^{(s,t)}$ mounting point of the Ith passive/active/hybrid control subsystem on $S^{(s)}$, $\mathbf{x}_I^{(s,t)} \in V^{(s)}$

$\mathbf{x}_I^{(t,s)}$ mounting point of the Ith passive/active/hybrid control subsystem on $S^{(t)}$, $\mathbf{x}_I^{(t,s)} \in V^{(t)}$

X_i global Cartesian co-ordinates

$X_i^{(s)}$ global co-ordinates of $S^{(s)}$

$\alpha_{Ii}^{(s,t)}$ unit directional cosine vector in the local co-ordinate system along which the Ith control subsystem are mounted between $S^{(s)}$ and $S^{(t)}$

$\tilde{\alpha}_{Ij}^{(s,t)}$ unit directional cosine vector in the global co-ordinate system along which the Ith control subsystem are mounted between $S^{(s)}$ and $S^{(t)}$

$\beta_{Ji}^{(s,0)}$ unit directional cosine vector in the local co-ordinate system along which the Jth sky-hook control subsystem are mounted on $S^{(s)}$

$\tilde{\beta}_{Ji}^{(s,0)}$ unit directional cosine vector in the local co-ordinate system along which the Jth sky-hook control subsystem are mounted on $S^{(s)}$

$\Gamma^{(s)}$ boundary of $S^{(s)}$, $\Gamma^{(s)} = S_u^{(s)} \cup S_T^{(s)}$

δ Kronecker delta

$\varepsilon_{kl}^{(s)}$ strain tensor of $S^{(s)}$

$\eta^{(s)}$ damping loss factor of $S^{(s)}$

v_i unit vector along outer normal of S_T

$\mathbf{v}^{(s)}$ unit vector along outer normal of $S^{(s)}$

$\mu^{(s)}$ the Poisson ratio of $S^{(s)}$

$\theta_{ij}^{(s)}$ transformation tensor from local system $o^{(s)}$-$x_1^{(s)}x_2^{(s)}x_3^{(s)}$to global co-ordinate system O-$X_1X_2X_3$

$\rho^{(s)}$ mass density of $S^{(s)}$

$\sigma_{ij}^{(s)}$ complex stress tensor of $S^{(s)}$

$\varphi_{in}^{(s)}$ retained the nth natural mode shape vector of $S^{(s)}$

$\mathbf{\Phi}_i^{(s)}(\mathbf{x})$ mode shape vector matrix of $S^{(s)}$ $(= [\varphi_{i1}^{(s)}, \varphi_{i2}^{(s)}, \ldots, \varphi_{iN^{(s)}}^{(s)}])$

$\Pi^{(s)}$ strain energy of $S^{(s)}$

$\boldsymbol{\omega}^{(s)}$ vector of natural frequency of $S^{(s)}$

Ω frequency of exciting forces

i, j, k subscripts $(=1, 2, 3)$ of a tensor, obeying the summation convention

I subscript to identify mountings in example $(=1, 2, 3, 4)$

(s) superscript $(=1, 2, \ldots, N)$, substructure identification number

(s, t) superscripts $(t \in H^{(s)}, s \notin H^{(s)})$, to identify any two substructures coupled by passive/active control subsystem

$(s, 0)$ superscript $(=1, 2, \ldots, N)$, to identify any substructure with sky-hook control subsystem

$\dot{(\,)}$ time derivative of $(\,)$

$(\,)_{,i}$ $= \partial(\,)/\partial x_i$

$(*)$ conjugate of a complex variable

$[\,]^{\mathrm{T}}$ transpose of a matrix

References

[1] L. Meirovitch, Dynamics and Control of Structures, Wiley, New York, 1990.

[2] C.R. Fuller, S.J. Elliott, P.A. Nelson, Active Control of Vibration, Academic Press, London, 1996.

[3] G.W. Housner, L.A. Bergman, T.K. Caughey, A.G. Chassiakos, R.O. Claus, S.F. Masri, R.E. Skelton, T.T. Song, B.F. Spencer, J.T.P. Yao, Structural control: Past, present, and future, Journal of Engineering Mechanics 123 (1997) 897–971.

[4] W.T. Thomson, Theory of Vibration with Applications, 3rd edition, Prentice-Hall, Englewood Cliffs, NJ, 1988.

[5] C.M. Harris (Ed.), Shock and Vibration Handbook, McGraw Hill, New York, 1988.
[6] Y.P. Xiong, K.J. Song, Power flow transmission influenced by vibration source impedance in a compound system, Chinese Journal of Acoustics 15 (1996) 314–318.
[7] M.D. Jenkins, P.A. Nelson, R.J. Pinnington, S.J. Elliott, Active isolation of periodic machinery vibrations, Journal of Sound and Vibration 166 (1993) 117–140.
[8] D.J. Leo, D.J. Inman, A quadratic programming approach to the design of active-passive vibration isolation systems, Journal of Sound and Vibration 220 (1999) 807–825.
[9] T.E. Pare, J.P. How, Hybrid H_2 control design for vibration isolation, Journal of Sound and Vibration 226 (1999) 25–39.
[10] S. Mahajan, R. Redfield, Power flow in linear active vibration isolation systems, Journal of Vibration and Acoustics, Transaction of the American Society of Mechanical Engineers 120 (1998) 571–578.
[11] J.Q. Pan, C.H. Hansen, Active control of power flow from a vibrating rigid body to a flexible panel through two active isolators, Journal of the Acoustical Society of America 93 (1993) 1947–1953.
[12] P. Gardonio, S.J. Elliott, R.J. Pinnington, Active isolation of structural vibration on a multiple-degree-of-freedom system, Part II: effectiveness of active control strategies, Journal of Sound and Vibration 207 (1997) 95–121.
[13] D. Sciulli, D.J. Inman, Isolation design for a flexible system, Journal of Sound and Vibration 216 (1998) 251–267.
[14] M. Serrand, S.J. Elliott, Multichannel feedback control for the isolation of base-excited vibration, Journal of Sound and Vibration 234 (2000) 681–704.
[15] S.M. Kim, S.J. Elliott, M.J. Brenan, Decentralized control for multichannel active vibration isolation, IEEE Transaction on Control Systems Technology 9 (2001) 93–100.
[16] C.E. Kaplow, J.R. Velman, Active local vibration isolation applied to a flexible space telescope, American Institute of Aeronautics and Astronautics Journal of Guidance and Control 3 (1980) 227–233.
[17] K.B. Scribner, L.A. Sievers, A.H. Von Flotow, Active narrow-band vibration isolation of machinery noise from resonant substructure, Journal of Sound and Vibration 167 (1993) 17–40.
[18] W.W. Clark, H.H. Robertshaw, Force feedback in adaptive trusses for vibration isolation in flexible structures, Journal of Vibration and Acoustics, Trans American Society of Mechanical Engineers 119 (1997) 365–371.
[19] P. Gardonio, S.J. Elliott, Passive and active isolation of structural vibration transmission between two plates connected by a set of mounts, Journal of Sound and Vibration 237 (2000) 483–511.
[20] D. Margolis, Retrofitting active control into passive vibration isolation systems, Journal of Vibration and Acoustics, Transactions of the American Society of Mechanical Engineers 120 (1998) 104–110.
[21] Y.P. Xiong, J.T. Xing, W.G. Price, Active control of bridge vibrations considering the vehicle-bridge dynamic interactions, Proceeding of the Asia-Pacific Vibration Conference 2 (1999) 1227–1232.
[22] Y.P. Xiong, Passive and active control of power flow applied to flexible coupling systems and structures, The Development of Vibration Engineering in China for the Next Century, China Astronautics Press, Beijing, pp. 79–90 (1999) (in Chinese).
[23] Y.P. Xiong, J.T. Xing, W.G. Price, Hybrid active and passive control of vibratory power flow in flexible isolation systems, Shock and Vibration 7 (2000) 139–148.
[24] Y.P. Xiong, J.T. Xing, W.G. Price, Power flow analysis of complex coupled systems by progressive approaches, Journal of Sound and Vibration 239 (2001) 275–295.
[25] Y.C. Fung, A First Course of Continuum Mechanics, 2nd edition, Prentice-Hall, Englewood Cliffs, NJ, 1977.
[26] H.T. Banks, Z.H. Luo, L.A. Bergman, D.J. Inman, On the existence of normal modes of damped discrete-continuous systems, Journal of Applied Mechanics 65 (1998) 980–989.
[27] R.E.D. Bishop, D.C. Johnson, The Mechanics of Vibration, Cambridge University Press, Cambridge, 1960.
[28] H.G.D. Goyder, R.G. White, Vibrational power flow from machines into buildup structures, part I: introduction and approximate analysis of beam and plate-like foundations, Journal of Sound and Vibration 68 (1980) 59–75.
[29] J.T. Xing, W.G. Price, A power-flow analysis based on continuum dynamics, Proceedings of Royal Society London A 455 (1999) 401–436.
[30] Y.C. Fung, A First Course in Continuum Mechanics, Prentice-Hall, Englewood Cliffs, NJ, 1977.
[31] R. Courant, D. Hilbert, Methods of Mathematical Physics, Interscience, New York, 1962.
[32] K.J. Bathe, Finite Element Procedures in Engineering Analysis, Prentice-Hall, Englewood Cliffs, NJ, 1982.
[33] J.L. Merian, L.G. Kraige, Engineering Mechanics, Dynamics, Wiley, New York, 1998.